THE LOCALIZATION OF BRANCHIAL CARBONIC ANHYDRASE IN THE SHARK, *SQUALUS ACANTHIAS*

by

Jonathan Mark Wilson

B.Sc., The University of British Columbia, 1993

A THESIS SUBMITTED IN PARTIAL FULFILLMENT OF

THE REQUIREMENTS FOR THE DEGREE OF

MASTER OF SCIENCE

in

The Faculty of Graduate Studies

(Department of Animal Science)

We accept this thesis as conforming to the required standard

The University of British Columbia

July 1995

In presenting this thesis in partial fulfilment of the requirements for an advanced degree at the University of British Columbia, I agree that the Library shall make it freely available for reference and study. I further agree that permission for extensive copying of this thesis for scholarly purposes may be granted by the head of my department or by his or her representatives. It is understood that copying or publication of this thesis for financial gain shall not be allowed without my written permission.

Department of ANIMAL SCIENCE

The University of British Columbia
Vancouver, Canada

Date OCT 2ND 1995

ABSTRACT

Differences in gill function, pattern of CO_2 elimination and ion /acid-base regulation, between elasmobranchs and teleosts are expected to be reflective of differences in the pattern of carbonic anhydase (CA) distribution within the gills of these groups. The distribution of branchial CA was investigated in the spiny dogfish, *Squalus acanthias*, using immunolocalization techniques, as well as *in situ* and *in vivo* measurements of pH disequilibrium states in post-branchial saline and blood, respectively. Biochemical and immunolocalization techniques were used to determine if V-type H^+-ATPase was present in the gills of dogfish. In addition, the cellular distribution of H^+-ATPase in the gill was determined in fresh and sea water adapted trout, *Oncorhynchus mykiss*, using immunocytochemical techniques in order to compare its distribution with that of CA in the trout.

Branchial CA in the dogfish is distributed throughout the outer epithelial cells and pillar cells. This pattern of CA distribution suggests a role in facilitating diffusion of CO_2 and in ion / acid-base regulation. The lack of a post-branchial pH disequilibrium in the *in situ* saline perfused gill preparation suggests that CA is available extracellularly along the blood lumen side of the pillar cell membrane to accelerate the HCO_3^- dehydration reaction, thus augmenting CO_2 elimination. The post-branchial pH decrease (acidosis) measured under control conditions *in vivo* provides equivocal evidence for the *in situ* finding.

In dogfish H^+-ATPase was localized to a subpopulation of mitochondria-rich (MR) cells in the interlamellar region. There was also significant N-ethymaleimide (NEM) sensitive ATPase activity (0.116 ± 0.026 μmol $P_i \cdot mg^{-1}$ protein $\cdot h^{-1}$) in crude gill homogenates. The immunolocalized MR cells may function in ion / acid-base regulation. In the trout, H^+-ATPase was localized to the apical membrane and subapical vesicles in epithelial pavement and mitochondria-rich cells was confirmed. The apical distribution gradient of the pump is remarkably similar to the distribution found for CA in trout.

TABLE of CONTENTS

List of Figures

List of Tables

Acknowledgments

The work presented here would not have been possible without the help and support of a number of people. I would first like to thank George Iwama, my supervisor, who provided me with this research opportunity and a place to call home. Cheers to Dave Randall and Wayne Vogl without whose help I would surely have been a lost cause. And to the above mentioned as well as Colin Brauner thanks for the fruitful discussions which have led to the evolution of this manuscript which you may (or may not) be contemplating giving a read. Also thanks to Dave Pfieffer and Robert Forsyth for help with the morphological and gel work, respectively. In addition, the physiological experiments on the dogfish would not have been possible without the technical assistance of Joëlle Harris. Thanks again to the above mentioned people as well as the rest of the Iwamites, Randallizers, and members of the Department of Anatomy for creating the positive environment in which to work (hence exist). In a moment quiet reflection I would like to acknowledge the sacrifice of the many dogfish and trout who participated in this study. Thanks also to those for providing and caring for them (Ellen Teng, John Boom, and Dwayne). Thanks also to Kathleen Gilmour, Steve Perry and Chris Wood for providing the gill tissue for the ATPase assays in the eleventh hour. Finally, I would like to thank NSERC Canada for providing me with the dosh that sustained me through the course of my studies. Lastly, a note to Jenn. I made it. Too bad we didn't. And so it goes.

INTRODUCTION

The majority of CO_2 produced in the tissues of fishes is transported to the gills as HCO_3^- in the plasma and H^+ buffered by the haemoglobin in the erythrocytes (see reviews: Perry 1986; Swenson 1990). During the blood's transit through the gill, molecular CO_2 diffuses along its concentration gradient out into the water where it is quickly carried away. This loss of CO_2 from the blood compartments (erythrocyte and plasma) disrupts the chemical ($CO_2 \leftrightarrow HCO_3^- + H^+$) status established during transit to the gills (Figure 1). Additional CO_2 is produced from the rapid dehydration of HCO_3^- by carbonic anhydrase (CA, carbonic dehydratase, EC 4.2.1.1) within the erythrocyte. The subsequent rapid depletion of intracellular HCO_3^- drives HCO_3^- influx via a Cl^- / HCO_3^- exchanger. In most vertebrates, oxygenation of the haemoglobin causes a release of (Bohr) protons from the haemoglobin (Jensen 1989). The Bohr protons 'boost' the rate of HCO_3^- dehydration within the erythrocyte (Haldane effect). This cascade of events maintains the blood P_{CO2}, hence the diffusion gradient and the rate of CO_2 elimination. The contribution of the plasma HCO_3^- dehydration reaction to total CO_2 excretion is limited by the plasma availability of CA and H^+ (Swenson 1990).

In dogfish the Haldane effect is functionally absent (Jensen 1989) and erythrocyte CA activity is 1/12 of that found in trout (Maren *et al.* 1980) yet efficient CO_2 excretion is maintained (Wood *et al.* 1994). The possibility of another mechanism to augment CO_2 elimination, in particular the role of branchial CA is investigated in the present study. Branchial CA can augment CO_2 excretion by accelerating the HCO_3^- dehydration in the

plasma (Bidani and Crandall 1988), and facilitating diffusion of CO_2 through the epithelium (Enns and Hill 1983) in addition to providing counter ions for ion / acid-base regulation (Perry and Laurent 1990). The ability of CA to perform these functions depends on its location and availability. To accelerate reactions in the plasma, CA would need to be distributed extracellularly along the blood side of the endothelial or pillar cell[1] membrane. To provide HCO_3^- and H^+ for acid-base/ ion regulation and to facilitate CO_2 diffusion CA would need a cytoplasmic distribution. The presence of CA in sharks and teleost gills has been demonstrated using biochemical (Hodler *et al.* 1955), pharmacological (Perry *et al.* 1982; Swenson and Maren 1987; Swenson *et al.* 1995), and histochemical/ immunocytochemical techniques (Dimberg 1981; Lacy 1983; Rahim *et al.* 1988; Conley and Mallatt 1987). These techniques have also been valuable in providing information about the location of CA in lungs and gills of mammals and teleost fishes, respectively. The majority of CA activity is cytoplasmic in both groups (Henry *et al.* 1986, 1988) but is available to the plasma of mammals (review Bidani and Crandall, 1988) and unavailable to the plasma of teleosts (Perry *et al.* 1982; Rahim *et al.* 1988; Henry *et al.* 1988). The cytoplasmic CA activity in the trout gill epithelium is distributed greater apically and less toward the basolateral membrane (Rahim *et al.* 1988).

Modulations of ventilation used effectively by terrestrial animals to correct acid-base imbalances are not available to fish because oxygen uptake rather than CO_2 excretion drives ventilation (O_2 content in water 1/10 of air; see review Heisler 1988). Instead, aquatic animals utilize gill epithelial transport proteins (e.g. H^+-ATPase, Na^+/H^+

[1] Pillar cells are morphologically distinct from endothelial cells. Caveolae and Weibel-Palade bodies which characterize endothelial cells are rare and absent, respectivley, in pillar cells (see Laurent 1984).

antiporter, Cl^-/ HCO_3^- antiporter) to regulate acid-base balance. Branchial CA is important in providing intracellular H^+ and HCO_3^- for these transporters (Perry and Laurent 1990). In dogfish, it is known that the gill is the site of H^+ excretion but the mechanism remains undefined (see Heisler 1988). The elimination of salt (NaCl) in marine fish is preformed by transport proteins in the gills of teleosts and in the rectal gland of sharks (Riordan *et al.* 1994; Evans 1993).

Differences in gill function, pattern of CO_2 elimination and ion /acid-base regulation, between elasmobranchs and teleosts are expected to be reflective of differences in the pattern of CA distribution within the gills of these groups. In the present study I hoped to elucidate the branchial distribution of CA using immunolocalization techniques, and *in situ* and *in vivo* measurements of disequilibrium states in post-branchial saline and blood, respectively. The premise of measuring the *in situ* post-branchial pH disequilibrium state was to determine if CA was available to accelerate the HCO_3^- dehydration reaction in the plasma, hence bring the reaction to equilibrium. The infusion of bovine CA and acetazolamide (ACTZ), a potent CA inhibitor (Maren 1984), were used as positive and negative controls, respectively. *In vivo* stopped-flow measurements were made to verify the *in situ* evidence for the presence of extracellular branchial CA. The direction of the *in vivo* post-branchial pH changes can be used to indicate the presence or absence of a branchial CA component to CO_2 reactions (Crandall and Bidani 1981). Again, infusions of bovine CA and ACTZ were used as positive and negative controls, respectively.

To ascertain whether a proton pump (H^+-ATPase) was available for acid-base regulation in elasmobranchs I localized activity using immunolocalization techniques as well as measured N-ethymaleimide (NEM) sensitive ATPase activty in gill homogenates using the method of Lin and Randall (1993). Specificity of antibodies was confirmed with appropriate controls as well as Western Blotting. To make a comparison between the detailed distribution of trout CA demonstrated by Rahim *et al.* (1988) and Perry and Laurent (1990), the H^+-ATPase in the gills of trout was also determined using an immunoelectron microscopic technique.

Figure 1. Schematic representation of CO_2 transfer in the gills of an elasmobranch fish. Note the possible contribution of carbonic anhydrase (CA) to facilitated diffusion, acid-base regulation, and HCO_3^- dehydration in the plasma and the erythrocyte (RBC). The Haldane effect is considered minor or absent. Other abbreviations and symbols: Haemoglobin (Hb), Protein (Prot), transmembrane ion transport proteins (O) (eg. Cl^-/ HCO_3^- antiporter, H^+-ATPase, Na^+/H^+ antiporter)

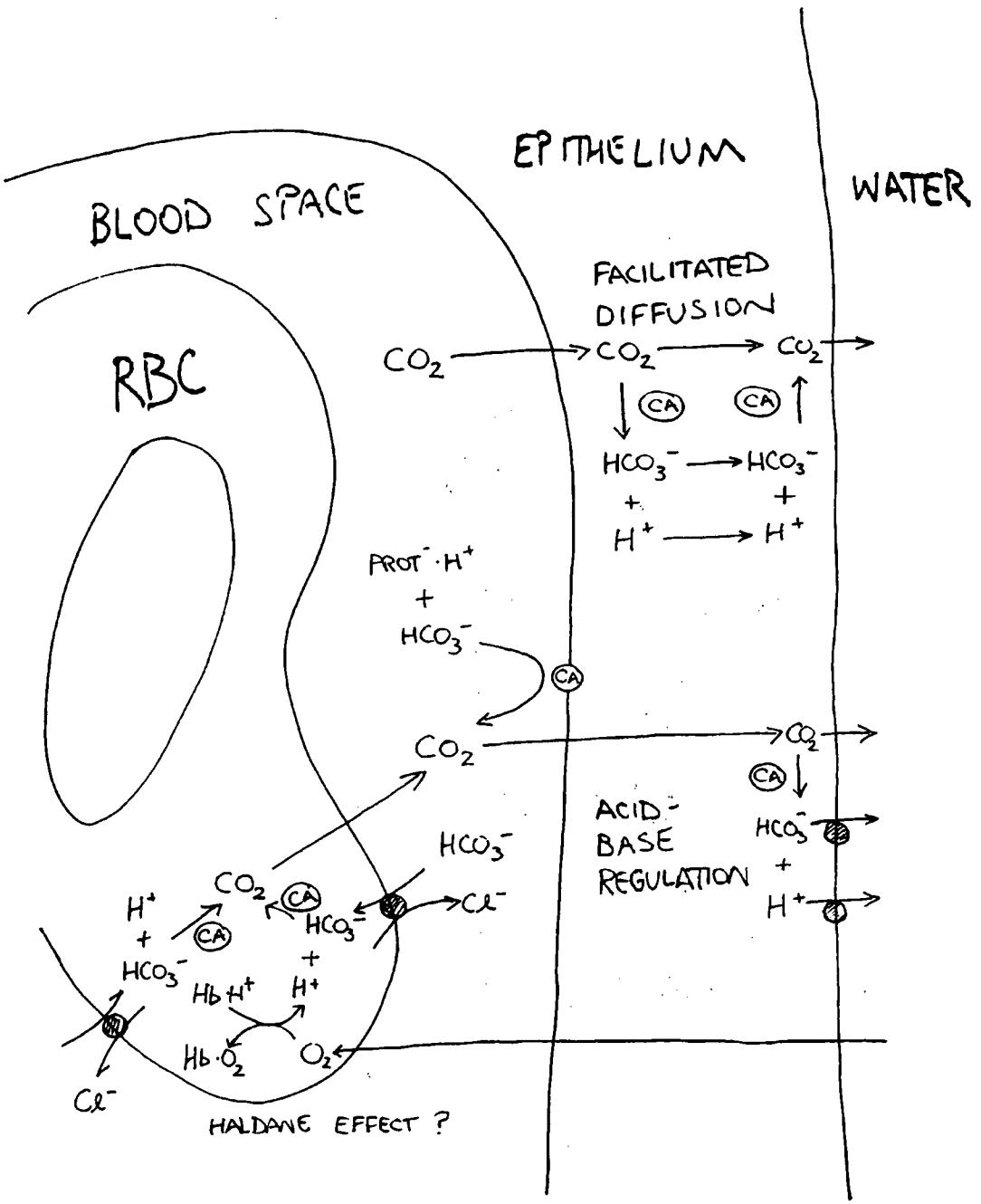
BLOOD SPACE
EPITHELIUM
WATER
RBC
FACILITATED DIFFUSION
CO_2
CO_2
CO_2
CA
CA
HCO_3^-
HCO_3^-
+
+
H^+
H^+
$PROT^- \cdot H^+$
+
HCO_3^-
CA
CO_2
CO_2
CA
ACID-BASE REGULATION
HCO_3^-
+
H^+
HCO_3^-
Cl^-
H^+
+
CA
CO_2
CA
HCO_3^-
+
HCO_3^-
$Hb H^+$
H^+
$Hb \cdot O_2$
O_2
Cl^-
HALDANE EFFECT ?

MATERIALS and METHODS

Animals

Dogfish, *Squalus acanthias*, were obtained from commercial shrimp fishermen and housed in flow through circular tanks at the Bamfield Marine Station (Bamfield, British Columbia). Water temperature remained constant at 11°C during the experiment. Mean body mass (mean ± SEM (n)) was 1.38 ± 0.17 kg (30). Rainbow trout, *Oncorhynchus mykiss*, were obtained from West Creek Trout Farm (Aldergrove, British Columbia) and housed in flow through circular tanks provided with either fresh or sea water (~12°C). Mean body mass was 0.375 ± 0.062 kg (8). In this study trout were used only for immunocytochemical localization of H^+-ATPase.

Dogfish Head Preparation

Surgery

Dogfish were injected by cardiac puncture with 5 ml (50 IU · ml^{-1}) heparinized saline[1] (Forster *et al.* 1972) 30 min prior to surgery. Each fish was euthanized with MS-222 (tricaine methanesulphonate; Syndel, Richmond B.C.), the cardiac cavity opened, and the ventral aorta (VA) cannulated with a 'Y' connector (Nalgene). The head was immediately perfused with 30 ml of heparinized saline to flush out erythrocytes from the gills. The head was then detached from the rest of the body and placed in a flowing seawater bath (dorsal side down) and the dorsal aorta (DA) was cannulated with

[1] containing 70 mM TMAO (Trimethylamine oxide)

polyethylene tubing (PE 280/ PE 190). The gills were irrigated with seawater and the VA perfused via the 'Y' connector with saline in a state of disequilibrium. (see Figure 2)

Protocol

Saline 'A' (acidic, 3 mM KH_2PO_4, no $NaHCO_3$) was mixed with saline 'B' (basic, 20 mM $NaHCO_3$) and perfused the dogfish head via the VA at an estimated rate of 1.5 $l \cdot h^{-1}$ (Kent and Pierce 1978). To monitor the disequilibria in saline, pH electrodes were placed in series 1.) pre-gill immediately after saline A and B mixing (pH and reference micro flow through electrodes; Microelectrodes Inc.), and post-gill, 2.) proximally (combination electrode, Fisher Scientific) and 3.) distally (combination electrode Orion Inc.). Electrodes were coupled to Radiometer-Copenhagen PHM71, PHM84 and PHM64 pH meters, respectively. Saline was drawn from the DA past the post-gill electrodes at 12 ml $\cdot$ min^{-1} with a peristaltic pump (Piper Pump). The transit time from the DA to the proximal electrode was approximately 6 s. The transit time from the proximal to the distal electrode was 1 min 23 s. Combination electrodes were housed in (1 ml) thermostatted chambers (11°C) mixed by micro teflon stir bars. Electrodes were calibrated with pH 6.38 and 7.04 standards (Radiometer-Copenhagen).

Readings were not taken until pH values displayed on the meters had stabilized (10 to 20 min post surgery). Treatments consisted of a control period followed by a CA infusion (10 000 IU $\cdot$ kg^{-1} bovine CA II, Sigma St. Louis MO) period and an acetazolamide (ACTZ) infusion (10^{-4} M sodium acetazolamide, Sigma) period. Readings were recorded manually every minute for 5 min in each treatment. The first readings for the CA and ACTZ groups were taken 5 min after the start of each respective

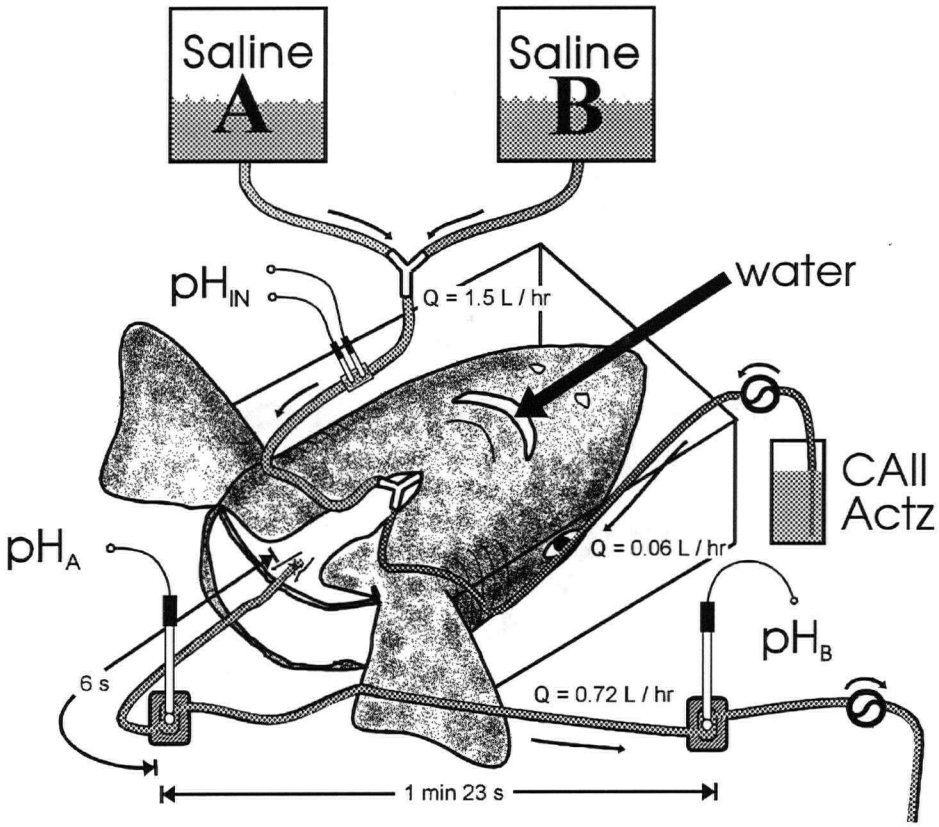

Figure 2. Schematic setup of saline purfused dogfish head preparation. Saline A (acidic) and B (basic) mix at 'Y' connector and have a net flow of 1.5 L / h. The mixed saline perfuses the head, cannulated at the ventral aorta. Concentrated stock solutions of CA or ACTZ are infused at this point by pump (~ 0.06 L / h). Saline is sampled (0.72 L /h) from the dorsal aorta (DA) and passed through two thermostatted (11°C) pH electrodes (pH_A and pH_B). pH_A is 6 s from the DA and 1min 23 s from pH_B.

treatment. The final concentrations of CA and ACTZ were achieved by using a peristaltic pump (Labconco) to infuse concentrated solutions into the 'Y' connector cannulating the VA.

The data are presented as pH_{IN} for pre-gill and pH_A and pH_B for the proximal and distal readings, respectively. The disequilibrium was measured as the pH difference between pH_A and pH_B.

On completion of the experiment the gills were examined for residual erythrocytes. No blood clotting was detected in the gills.

An experiment was conducted in which salines 'A' and 'B' were mixed in the experimental apparatus in the absence of a dogfish head. Saline and saline with 10^{-4} M ACTZ resulted in a detectable disequilibrium state following mixing (0.100 pH units). Saline with CA resulted in a negligible disequilibrium (0.001 pH units).

Dogfish Caudal Extracorporeal Loop

Surgery

Dogfish were anaesthetized with MS-222 (1:10000), weighed, and killed by decerebration. The tail was severed posterior to the pelvic fins (Piiper and Schumann 1967) and a polyethylene (PE) 190 tubing sheathed in a short section of PE 280 was advanced through the dorsal aorta to a point 5 to 10 cm posterior to the head. A peristaltic pump (Labconco) was used to circulate blood through a micro flow through pH and reference electrode (Microelectrodes Inc.) coupled to a pH meter (PHM 84, Radiometer-Copenhagen). The caudal vein was cannulated with PE 280 through which

blood was returned to the body creating a closed extracorporeal loop. Blood sinuses were plugged with tissue paper and a tourniquet was applied to minimize blood loss. The flow through the extracorporeal loop was estimated at 2.9 ml · min^{-1} and the transit time through the DA cannula (30 cm) to the pH electrode was estimated to be 7 s. The electrodes were calibrated with pH 6.923 and 7.469 precision buffers (S1500, and S1510, respectively; Radiometer-Copenhagen).

Haematocrit was monitored to assess blood loss, while plasma haemoglobin concentration was measured to determine erythrocyte lysis which may be attributed to blood passage through the extracorporeal loop. Haematocrit and plasma haemoglobin did not change significantly during the experiment.

Protocol

Fish were kept in a flowing seawater bath (ventral side down) and the gills were irrigated during a 30 min recovery period and during the experiment. Fish ventilated spontaneously (Swenson and Maren 1984). The stopped-flow method was used to evaluate equilibrium states of the blood. Three stop-flow measurements of 2 min each spaced by 2 min intervals were made per treatment. The half time of the uncatalyzed HCO_3^- dehydration is between 25 and 90 s at physiological pH and temperature (Perry, 1986). The treatments consisted of a control period, a bolus injection of CA II (10 000 IU / kg) followed by a 10 min mixing period after which measurements were made, and a bolus injection of ACTZ (10^{-4} M sodium acetazolamide) followed by three reading periods (0, 30, and 60 min post ACTZ infusion). The stopped-flow pH change was calculated as pH_{stop} - pH_{flow}.

Fixation Protocols

Dogfish gill samples were fixed for immunofluorescene labeling, immunogold labeling, and ultrastructural analysis. Samples were taken in the same manner but the fixation protocols differed as described below. Gills from freshwater and seawater adapted (6 wk) rainbow trout were sampled and processed on a separate occassion from the dogfish for immunogold localization of H^+-ATPase only.

Fish were euthanized by decerebration. Immediately thereafter, a portion of the second gill arch on the left side was excised and immersed in a dish of fixative. Tissue for immunofluorescence labeling was immersion fixed in 3% paraformaldehyde / 9% sucrose/ phosphate buffered saline (PBS, 150 mM NaCl, 5 mM KCl, 3.2 mM Na_2HPO_4, 0.8 mM KH_2PO_4) pH 7.3 for 1 h along with Hake liver. After washing in PBS, pieces of either gill or rectal gland were placed in sandwiches of liver. The sandwiches were placed in a mold with HistoPrep (Fisher) and immersed in liquid nitrogen (Pfeiffer and Vogl 1991). Blocks were stored in liquid nitrogen until sectioning.

Tissue for the EM studies, immunogold labeling and ultrastructural analysis were sampled at the same time. Tissue samples were divided before fixation and placed in appropriate fixatives. Tissue for immunogold labeling was fixed according to procedures outlined by Tokuyasu and Singer (1976). In short, a primary fixation with 3% paraformaldehyde/ 20 mM ethylacetimidate/ 9% sucrose / PBS pH 7.3 at 11°C. During this time the tissues were cut into small pieces. After 10 min the pieces of tissue were transferred to a glutaraldehyde fixative (3% paraformaldehyde/ 0.1% glutaraldehyde / PBS pH 7.3) to fix for 1 h (11°C to 23°C). After washing with PBS and 50 mM NH_4Cl /

PBS, the pieces of tissue were then dehydrated in an ethanol series and embedded in Unicryl (British BioCell) at low temperature (4 to -20°C). Blocks were polymerized with UV light at -20°C.

In addition to this fixation and embedding scheme that proved successful for trout, a glutaraldehyde free periodate-lysine-paraformaldehyde fix (McLean and Nakane 1974) and a simple 3% paraformaldehyde / PBS fixative were used. These tissues were embedded in either Unicryl (as above) or dehydrated in an ethanol series (to 70%) and polymerized in LR White at 60°C for 24 h.

Tissue for routine ultrastructural analysis was fixed with a Karvanosky (1965) type fixative (1.5% paraformaldehyde/ 1.5% glutaraldehyde/ 0.1M sodium cacodylate pH 7.3) for 2 h. After washing in 0.1M Sodium Cacodylate tissue were postfixed in reduced osmium (1.5% KFeAsO/ 1% osmium tetroxide) for 1 h at room temperature, washed with double distilled water (ddH_2O), and stained in 1% aqueous uranyl acetate for 1 h. Tissues were prepared for embedding in Epon 812 (PolyScience) by serial dehydrating with ethanol and polypropylene oxide.

Sectioning and Staining

Tissues prepared for immunofluorescence were sectioned in a cryostat at -20°C. Sections 8-10 μm thick were mounted on poly-lysine coated glass slides and fixed in acetone at -20°C for 5 min. Slides were then allowed to air dry.

Sections were rehydrated with 5% normal goat serum (NGS) / 0.1% bovine serum albumin (BSA) / TPBS (0.05% Tween-20 in PBS) pH 7.3 for 30 min. Sections were incubated with primary antibody in 1% NGS/ TPBS or the appropriate control

(normal rabbit serum (NRS) or buffer) at 37°C for 1 h. The primary antibodies were rabbit polyclonals against either CA II, or H^+-ATPase. After washing with 0.1% BSA/ TPBS, sections were incubated with goat anti-rabbit fluorescene isothiocynate (FITC) conjugated IgG (Sigma) at 37°C for 1 h. After washing with 0.1% BSA / TPBS, sections were mounted with VectaSheild (Vector Laboratories Inc., Burlingame, CA). Material was viewed with an Zeiss Axiophot photomicroscope fitted with filter sets for detecting FITC.

Mounted cryosections were also treated with trypsin (10, 50, or 100 μg/ml PBS) at 4°C for 5 min (Pan *et al.* 1993) in order to visualize H^+-ATPase staining in dogfish gill. The sections were blocked with 20% fetal bovine serum (FBS) before proceeding with the above described staining procedure.

Tissues prepared for immunogold labeling were sectioned on either a Potter-Blum or a LKB ultramicrotome. Thin sections were collected on carbon/formvar coated nickel grids. Sections were rehydrated on drops PBS/ 0.01 M glycine / 0.1% BSA / 5% NGS / 0.05% Tween-20. Sections were then incubated at rt with the (1:100) primary antibody, normal rabbit serum or buffer alone for 2 h (PBS / 0.01 M Glycine / 1% NGS). Grids were then gently washed with PBS / 0.01 M glycine / 0.1% BSA before being incubated for 1 hour with either secondary antibody (1:20) gold conjugate (10 nm) or buffer alone (PBS / 0.1% BSA / 0.05% Tween-20 / 5% FBS). After a gentle wash with PBS, sections were fixed with 2.0% glutaraldehyde / PBS. Finally grids were washed with ddH_2O and counter stained with saturated uranyl acetate (4 min) and lead citrate (4 min). Sections were viewed on a Phillips 300 TEM at 80 kV.

Western Blots

Crude gill homogenates were prepared from fresh gill tissue homogenized by sonication (4 x 20 s strokes) in buffer as described by Lin and Randall (1993; see below) or as described for the ATPase assay (see below). SDS-polyacrylamide electrophoresis (PAGE) was carried out under conditions described by Laemmli (1970). To optimize resolution in the expected molecular weight ranges 12.5% and 10% SDS-polyacrylamide running gels with 5% stacking gels were used for eventual probing for CA II (30 kDa) and H^+-ATPase (70 kDa), respectively (Blattler *et al.* 1972). Gels destined for CA II and H^+-ATPase probing were loaded with 5 μg and 5-100 μg protein per lane, respectively. Protein concentrations were determined using the method described by Bradford (1976) using a BSA standard. Electrophoresis was carried out on a vertical mini-slab apparatus (Bio-Rad, Richmond CA) at 75 V for 20 min then at 150 V for 1 h. Following electrophoresis, gels were equilibrated in transfer buffer (Bjerrum *et al.* 1986) and transferred to nitrocellulose membranes using a semidry transfer apparatus (Bio-Rad,) operated at 13 V for 20 minutes (Towbin *et al.* 1979). After transfer, blots for CA II probing were blocked in 2% skimmed milk tris buffered saline (TBS, 20 mM tris-HCl, 500 mM NaCl) / 0.08% sodium azide and blots for H^+-ATPase probing were either blocked (as above) or digested with trypsin (5, 10, or 20μg · ml TBS^{-1}) for 5 or 10 min at room temperature (rt) followed by blocking with 20% FBS (Pan *et al.* 1993). Blots for CA II probing were incubated for 1 h at rt with a polyclonal rabbit anti-avian (chick) CA II antiserum diluted 1:250 with 2% skimmed milk / TBS containing a protease inhibitor cocktail (0.5 μg · ml^{-1} leupeptin, 10^{-6} M pepstatin, 1 μg · ml^{-1} aprotinin, and

1mM PMSF (phenylmethylsulfonyl fluoride)). Blots for H^+-ATPase probing were incubated overnight at 4°C with a polyclonal rabbit anti-bovine H^+-ATPase antiserum diluted 1:1000 as above. After washing with TBS / 0.05% Tween-20, blots were incubated with either goat anti-rabbit IgG conjugated to alkaline phosphatase (AP) (1:6000) or horseradish peroxidase (HRP) (1:2000) for 1 h at rt. Following washing with TBS / 0.05% Tween-20, blots were respectively incubated with alkaline phosphatase buffer with BCIP (5-bromo-4-chloro-3-indolyl phosphate) and NBT (nitroblue tetrazolium; Sigma) (Blake *et al.* 1984) or enhanced chemiluminescence (ECL) (Amersham) for visualization of cross reactive bands. The latter detection method was used because of weakness of the signal. Images were digitalized and were enhanced (Adobe PhotoShop) while maintaining the integrity of the data.

ATPase Assay

Preparation of Homogenates

Dogfish were killed by an overdose of MS-222 and a gill arch was removed (n=7). The arches were rinsed with sea water and the filaments were scraped from the septum with a razor blade and quickly frozen on dry ice. Tissue were homogenized according to the proceedure of Zaugg (1982), modified by Lin and Randall (1993). Samples (~1 g) were thawed in 2 ml of ice cold homogenization buffer I (100 mM Tris-HCl, 300 mM sucrose, 2 mM EGTA (ethylene glycol-bis (β-aminoethyl ether) N,N,N',N'- tetraacetic acid), 1mM dithiothreitol, pH7.3) and homogenized with a motor driven Teflon-glass homogenizer on ice (20 strokes). The homogenate was diluted with

2 ml ddH_2O and centrifuged for 15 min in a clinical centrifuge at 3000g (4°C). The supernatant was discarded and the pellet resuspended by sonication (20 strokes) in 1 ml 6% CHAPS (3-[3-cholamidopropyl)-dimethylammonio]-1-propansulfonate; zwitterionic detergent) / homogenization buffer I. The homogenate was centrifuged as before but this time the supernatant was saved for measuring ATPase activity. Samples were stored at -80°C. Total protein was determined using the Bradford method (1976).

ATPase Actvity

Na^+-K^+-ATPase and H^+-ATPase activities were measured using the coupled-enzyme method of Scharschmidt *et al.* (1979) modified by Lin and Randall (1993). The assay was modified for use on a microplate reader. ATPase activty was measured under two conditions for each sample: 1.) 245 µl reaction mixture + 5 µl of crude homogenate, and 2.) 245 µl reaction mixture containing 1.0 mM NEM + 5 µl of crude homogenate. The reaction solution contained 125 mM Tris-HCl, 1.0 mM EGTA, 12.5 mM KCl, 5.0mM NaN_3 (azide), 2.0 mM oubain, 5.0 mM $MgCl_2$, 5.0 mM ATP (adenosine triphosphate), 2.5 mM PEP (phosphoenolpyruvate), 0.5 mM NADH (β-nicotinamide adenine dinucleotide, reduced), 10 units each of LDH (lactate dehydrogenase) and PK (pyruvate kinase). The reaction was monitored continuously at room temperature (25°C) on a ThermoMax (Molecular Devices Corporation) microplate reader at 340 nm. The N-ethymaleimide sensitive H^+-ATPase activty was calculated from the differences between 1.) and 2.). Activity was expressed as µmol Pi · mg^{-1} protein · h^{-1}.

Statistical Analysis

Data are presented as the mean ± 1 standard error of the mean. Data that met the assumptions of normality (Bartlett's test) and homogeneity of variance were analyzed by a one-way repeated measures analysis of variance (ANOVA). Data that failed to meet the parametric requirements, and could not be normalized through transformation were analyzed with the nonparametric Friedman's repeated measure ANOVA. These tests were used to analyze variance within treatments and then between treatments. Upon failure to detect significant variance within treatments (time effect), values for each fish over the treatment time courses were averaged and these means were used in treatment comparisons (Figures 3a, 3b, & 4b). In treatments (Figure 4a) in which significant variances within treatments were detected (time effect) and values could not be averaged for each fish over the treatment time courses, treatments were compared at each time point. The *post hoc* Student-Newman-Keuls (SNK) multiple comparison test was used to compare treatments in which significant variation was found. The calculated pH changes (Figures 3b, 4b) were also tested for significant difference from zero using single mean one or two tailed t-tests. The level of statistical significance was set at $P \leq 0.05$.

RESULTS

Head Preparation

Saline pH values recorded within each treatment (control, CA infusion, and ACTZ infusion) were found not to vary significantly with time and were subsequently averaged for each fish within each treatment time course for pH (pH_{IN}, pH_A, pH_B) and pH disequilibria (pH_B - pH_A) data. These mean values were compared between treatments. The pH_{IN} and pH_B values for control, CA, and ACTZ treatments did not vary significantly between treatments (Figure 3a). The pH_A value for the ACTZ treatment was significantly less than both control and CA treatments.

The pH disequilibrium (pH_B-pH_A) during the ACTZ treatment was significantly greater than zero, as well as both control and CA treatments (Figure 3b). Control and CA treatments did not differ significantly.

Caudal Extracorporeal Loop

Flowing blood pH values recorded during control and CA periods were found not to change significantly with time and were subsequently averaged for each fish within each treatment time course. The values were not, however, presented as single means because pH values recorded after ACTZ infusion were found to vary significantly with time. The post ACTZ infusion pH values were compared to the mean control and CA values. Addition of CA did not result in a significant change in arterial pH (7.718 ± 0.040) from the control (7.740 ± 0.039) (Figure 4a). Addition of ACTZ, however,

resulted in an immediate acidosis. Blood pH did start, however, to recover to pre-ACTZ levels after 40 min.

Disequilibria data were found not to vary with time within each treatment and were subsequently averaged for each fish within each treatment time course (Figure 4b). Blood pH showed a small but significant drop in the control measurement when compared to zero (no change). The control disequilibrium was not significantly different from the disequilibria after CA or immediately after ACTZ (ACTZ 0) treatments. Thirty minutes after the ACTZ bolus infusion (ACTZ 30), the disequilibrium was significantly greater than during the control period. One hour after the ACTZ infusion the disequilbrium (ACTZ 60) was significantly greater than during both the control and CA periods. When compared to zero (no change) all three ACTZ periods were significantly greater and the CA disequilibria was not significnatly different from zero.

Immunolabeling

Carbonic Anhydrase

The rabbit anti-chick CA II polyclonal antiserum cross reacted strongly with fixed, frozen dogfish gill sections. The immunofluorescent localization of CA in the branchial epithelium was seen in most outer epithelial cells but was of variable intensity and intracellular distribution (Figure 5a, 6a). The outer epithelial cells in the interlamellar space and along the base of secondary lamellae primarily had a diffuse cytoplasmic staining while some cells along the secondary lamellae had a more granular cytoplasmic staining pattern. Pillar cells showed an occasional positive signal in the cell body and

along the flanges. Immunofluorescence does not provide the necessary detail required to determine whether the pillar cell CA is available to the blood. Erythrocytes were also seen to label positively, the nuclei being indicated by their negative image in fluorescence. No nonspecific fluorescence was detected with control sections (5b, 6b-d).

The high resolution immunogold technique was employed to resolve the problem of detailed pillar cell localization but the attempts at immunogold labeling failed. The results from the three fixation regimes and two embedding protocols failed to produce labeling above background levels (results not shown).

H^+-ATPase

Immunofluorescent localization of H^+-ATPase proved successful only with prior trypsin digestion of cryosections (10, 50, and 100 $\mu g \cdot ml^{-1}$ trypsin) (Figure 7a ,8a). The level of specific staining did not show a noticeable increase with increased digestion but nonspecific staining did increase (Figure 7b, 8b). Specific labeling was restricted to cells of the interlamellar region in contact with the external milieu (Figure 7). The staining pattern within these interlamellar cells showed a low level general diffuse pattern with an intense granular apical signal. The nuclei can be visualized as a negative image in fluorescence and the cells generally have an ovoid shape. A morphological investigation of this region of the gill at the EM level indicated the presence of mitochondria-rich (MR) cells which possess a similar ovoid shape as the observed fluorescent cells as well as a supranuclear concentration of tubulovesicles (Figure 9). The insert shows the exposed surface of a MR cell flanked by pavement cells. Unlike seawater teleost MR cells, dogfish MR cells lack an apical crypt and a tubular system (see Laurent, 1984). The

morphological features used to characterize the MR cells are as described by Wright (1973) and Laurent and Dunel (1980). Another group of cells and cell fragments found in the inner epithelium (never in contact with the surface) also labeled positive for H^+-ATPase but also labeled in NRS incubated sections indicating they are not staining specifically (Figure 7).

The immunogold technique was attempted to determine the subcellular localization of H^+-ATPase in the MR cells. The use of the same alternative fixation and embedding protocols (as above) were also found unsuccessful (results not shown). Digestion of sections with trypsin was not attempted.

Immunogold localization of H^+-ATPase in Trout

Immunogold localization of H^+-ATPase in freshwater trout gill pavement (PVC) and MR cells (Figure 10). Gold particles can be seen to be associated with the apical plasma membrane of both cell types on the secondary lamellae and primary filament. Subapically, staining can be observed associated with vesicles. Control sections showed little appreciable staining (results not shown).

Western Blots

Western blot analysis with the CA II specific probe revealed a single band with an approximate molecular weight of 30 kDa in dogfish gill homogenate (Figure 11). The polyclonal CA II antibodies also cross reacted strongly with the bovine CA molecular weight marker (29.5 kDa).

The polyclonal H^+-ATPase antibodies cross reacted weakly with a band in the approximate 70 kDa size range from the crude homogenate from dogfish gill (Figure 12). The more sensitive ECL detection method was required to visualize bands. Trypsin treatment did not improve expression in the H^+-ATPase probed blots.

ATPase Assay

NEM sensitive H^+-ATPase activity from the crude gill homogenate of dogfish gills are presented in Table 1. NEM inhibited activity was 33% of the total ATPase and was significantly different from zero.

Figure 3. Dogfish head preparation. *In situ* heads were perfused with saline and the pH was measured from three points in the system (pregill, pH_{IN}, and post gill proximal, pH_A, and distal, pH_B) during control (Ctrl), carbonic anhydrase (CA) and acetazolamide (ACTZ) treatments. n = 10

A.) Mean pH_{IN} (hatched) and pH_A (no fill) and pH_B (solid black) for treatments. Arrows indicate the start of infusion of CA (10 000 IU · kg^{-1}) and ACTZ (10^{-4}M). The asterisk (*) indicates a significant difference from Ctrl and CA treatments. $P < 0.05$

B.) Mean pH disequilbria values (pH_B- pH_A) during control, CA and ACTZ treatments. The asterisk (*) indicates a significant difference from Ctrl and CA treatments, and zero. $P < 0.05$

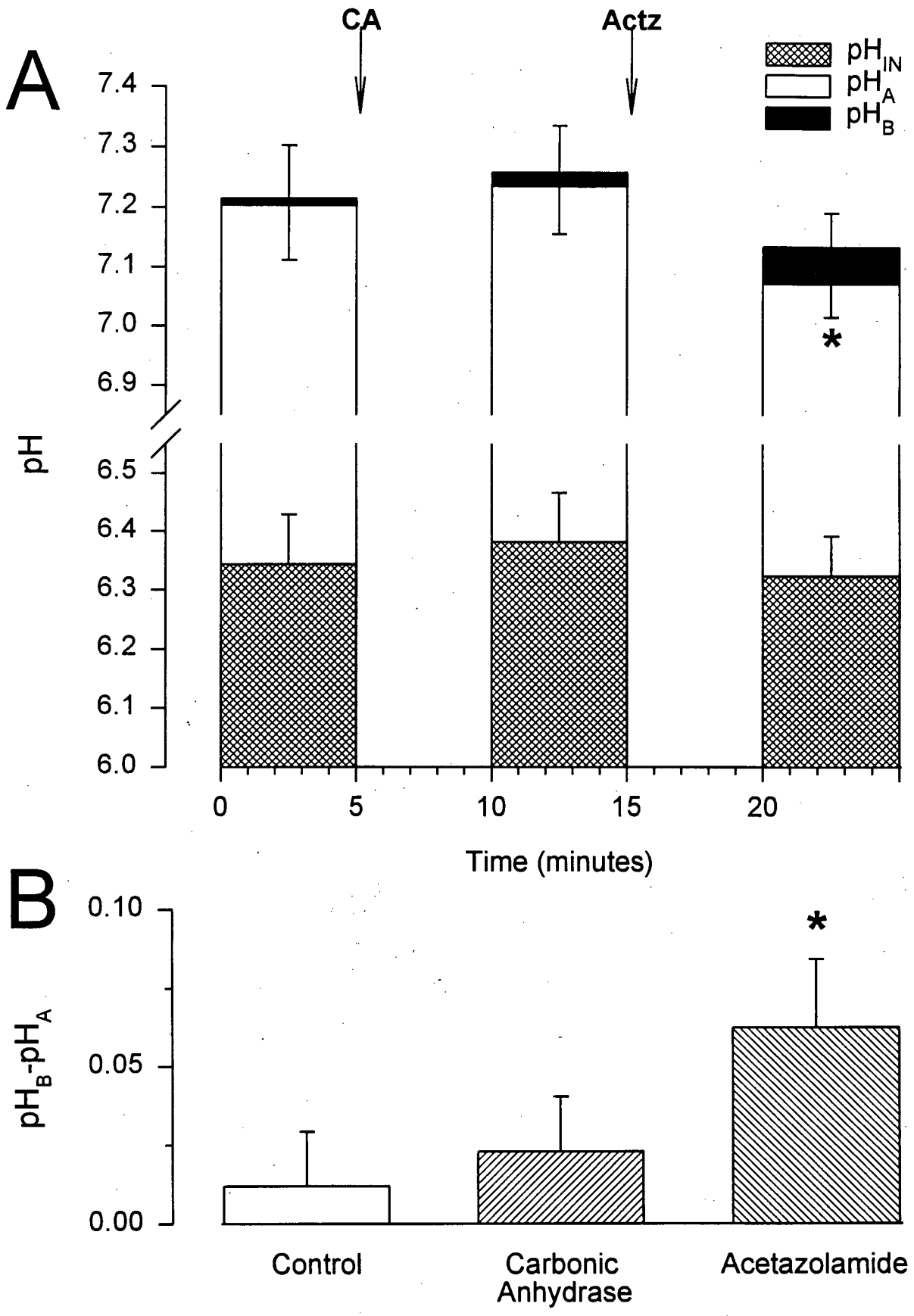
A
CA
Actz
pH_IN
pH_A
pH_B
7.4
7.3
7.2
7.1
7.0
6.9
6.5
6.4
6.3
6.2
6.1
6.0
pH
*
0
5
10
15
20
Time (minutes)
B
0.10
0.05
0.00
pH_B-pH_A
*
Control
Carbonic Anhydrase
Acetazolamide

Figure 4. Dogfish caudal extracorporeal loop. The arterial pH was measured *in vivo* with an extracorporeal loop during control (Ctrl), carbonic anhydrase (CA) and acetazolamide (ACTZ) treatment periods. The ACTZ treatment period is broken into three groups at 0 minutes (ACTZ-0), 30 minutes (ACTZ-30) and 60 minutes (ACTZ-60) post ACTZ infusion. n = 6

A.) pH measurements in the stopped (hollow) and flowing (solid) blood for Ctrl (circle), CA (square) and ACTZ (triangle, inverted triangle and diamond for ACTZ-0, ACTZ-30 and ACTZ-60, respectively) recording periods. Arrows mark times of bolus infusions of CA II (10 000 IU · kg^{-1}) and ACTZ (10^{-4}M). The asterisk (*) indicates a significant differences between mean Ctrl and ACTZ pH values. The number symbol (#) indicates a significant differences between mean CA and ACTZ pH values. ($P < 0.05$)

B.) Mean pH disequilibria values averaged for each fish over the recording periods, Ctrl, CA, ACTZ-0, ACTZ-30 and ACTZ-60. Bars with the same superscript do not differ significantly. Bars with an asterisk (*) are significantly differenent from zero. ($P < 0.05$)

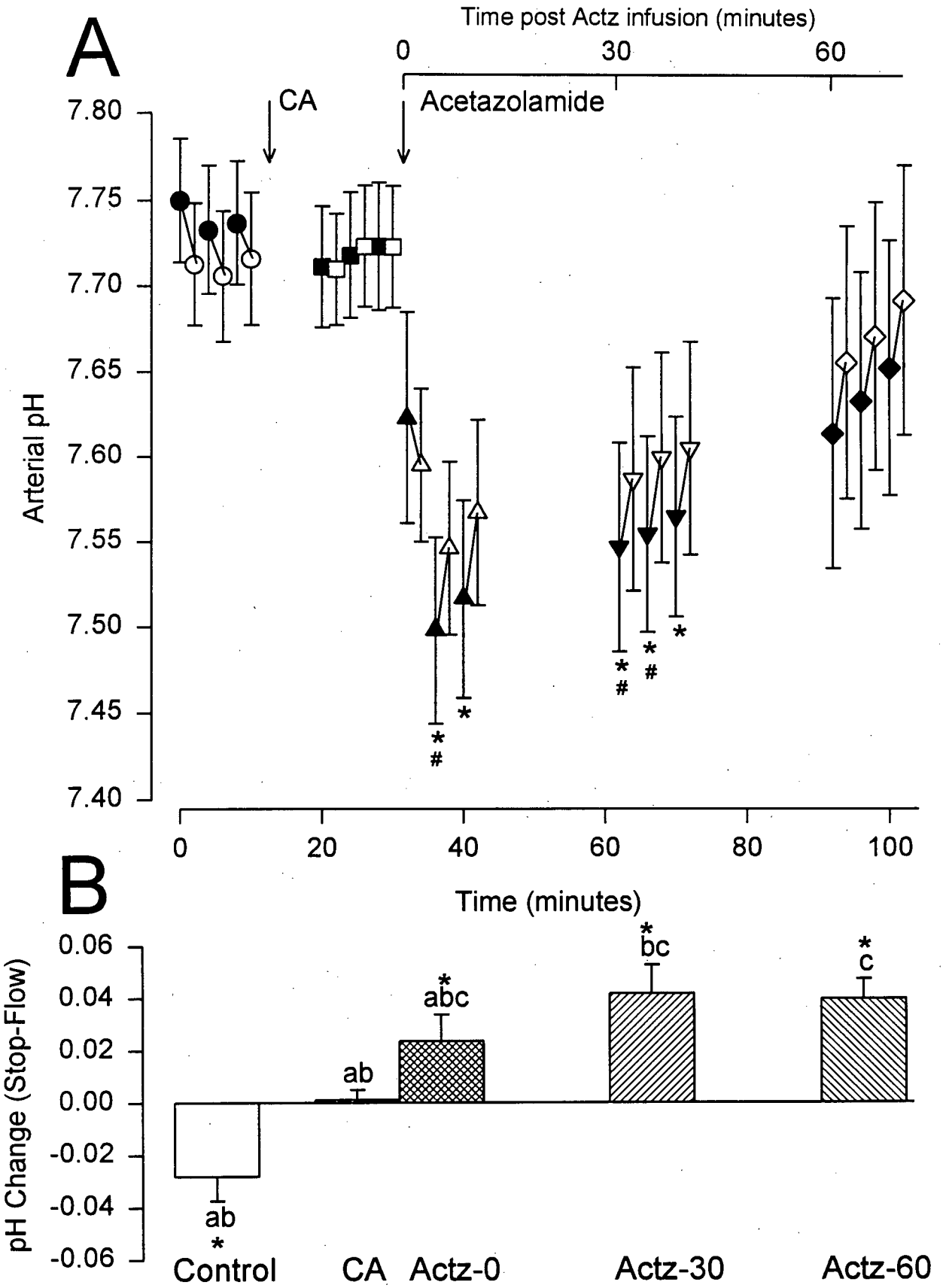
A
Time post Actz infusion (minutes)
0
30
60
CA
Acetazolamide
7.80
7.75
7.70
7.65
7.60
7.55
7.50
7.45
7.40
Arterial pH
0
20
40
60
80
100
Time (minutes)
B
0.06
0.04
0.02
0.00
-0.02
-0.04
-0.06
pH Change (Stop-Flow)
ab
abc
bc
c
Control
CA
Actz-0
Actz-30
Actz-60

Figure 5. Paired fluorescence and phase micrographs (**A** and **A'**, respectively) of immunochemically localized carbonic anhydrase in fixed frozen sections of dogfish gill. Positive staining can be seen in epithelial cells along the secondary lamellae and interlamellar space on the primary filament. The other pair of fluorescence and phase micrographs (**B** and **B'**, respectively) represent sections incubated with the normal rabbit serum (nrs) control. No specific staining is observed in these sections. Bar = 100 μm.

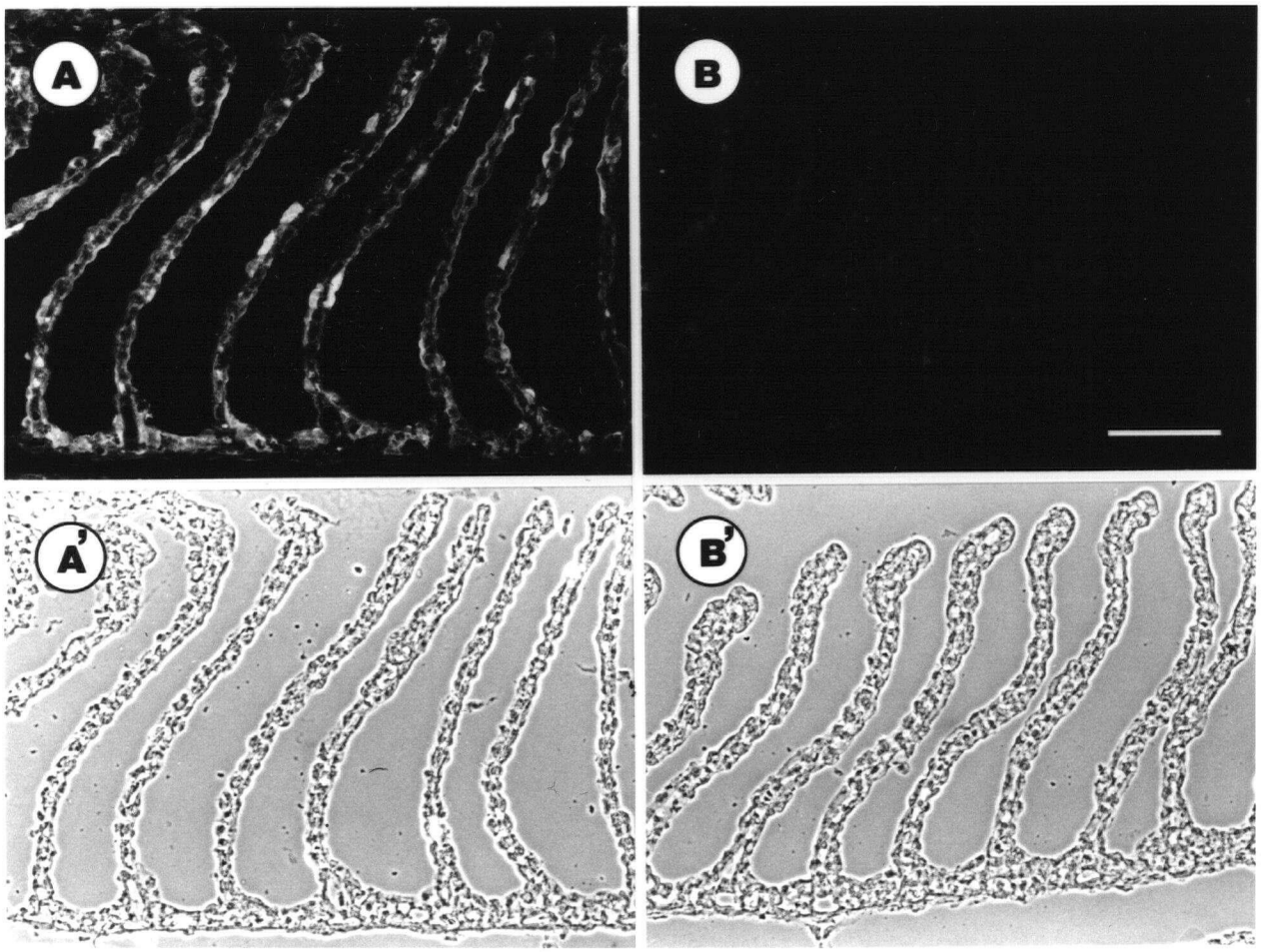
A
B
A'
B'

Figure 6. Carbonic anhydrase distribution in secondary lamellae of fixed frozen sections of dogfish gill using indirect immunocytochemistry. Either a general diffuse staining or a punctate staining pattern was observed in epithelial cells (Paired fluorescence and phase micrographs, **A** and **A'**, respectively). Red blood cells and pillar cells also display a positive signal (small arrow and small arrow head, respectively). No specific staining was observed in sections in which the specific primary antibody was replaced by either normal rabbit serum (**B** and **B'**), or buffer (**C** and **C'**), or in which both the primary and secondary antibodies were replaced by buffer (**D** and **D'**). Bar = 50 μm.

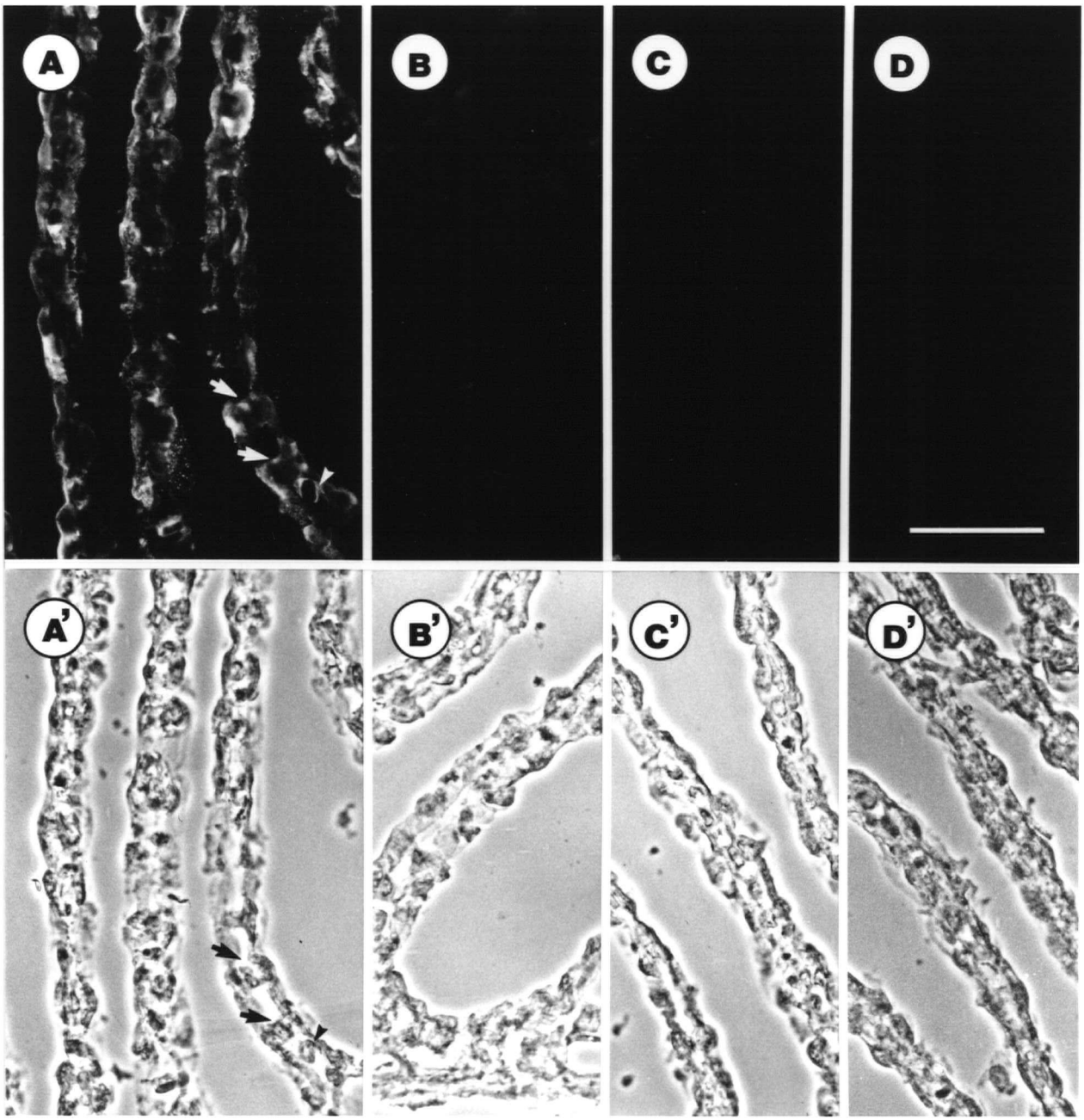
A
B
C
D
A'
B'
C'
D'

Figure 7. Paired fluorescence and phase micrographs (**A** and **A'**, respectively) of proton-ATPase distribution in fixed frozen sections of dogfish gill treated with trypsin (100μg · ml PBS^{-1}) for 5 min at 4°C. Specific staining can be seen in outer epithelial cells along the interlamellar space on the primary filament. Staining in cell/ cell fragments associated with blood spaces (arrow) is nonspecific because it is also present in the normal rabbit serum (nrs) control (**B** and **B'**). Predigestion of sections with trypsin results in a high level of background staining. Bar = 50 μm.

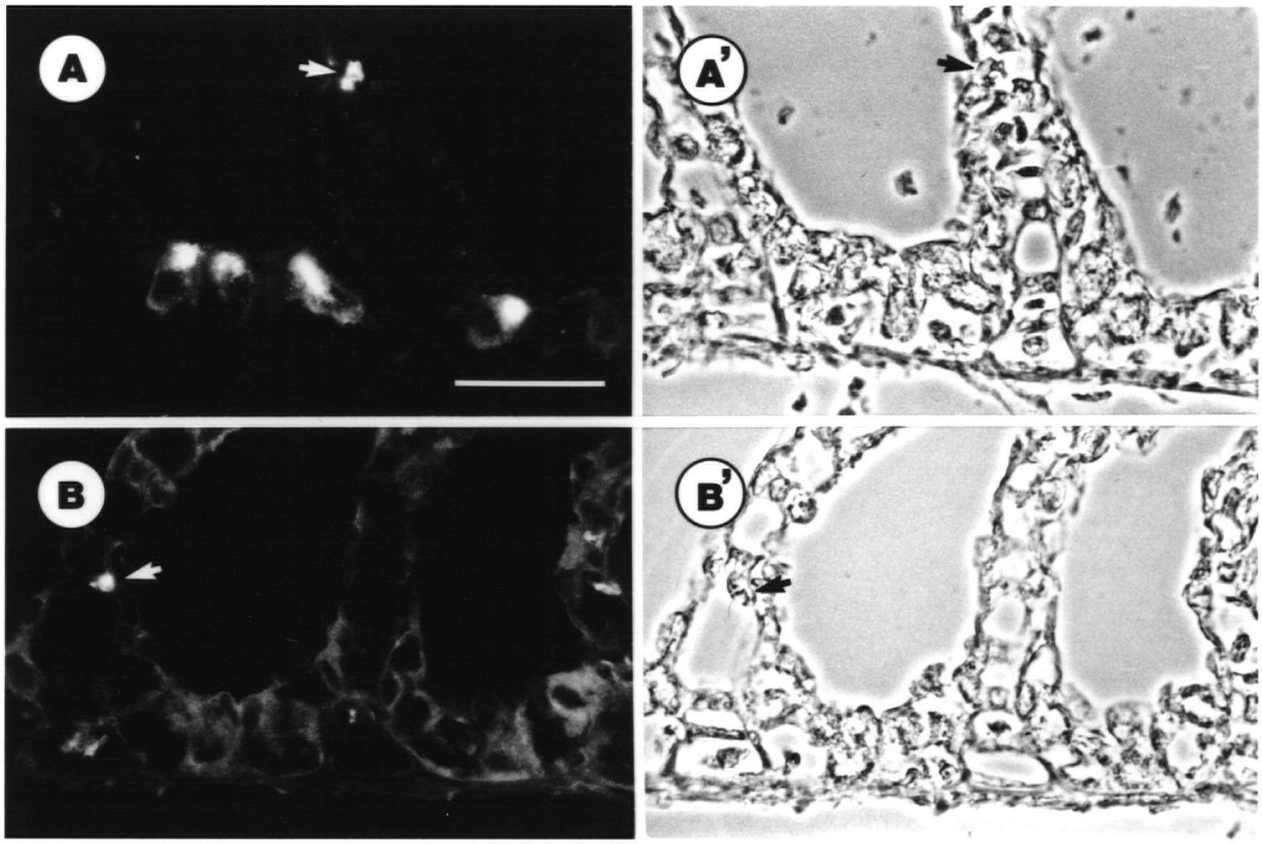
A
A'
B
B'

Figure 8. A control series for the immunofluorescence localization of proton-ATPase in fixed frozen sections of dogfish gill predigested with trypsin (50 μg · ml PBS^{-1}) for 5 min at 4°C. Micrographs are shown in pairs as seen under fluorescence and phase-contrast modes. Digested sections incubated with a proton-ATPase specific antiserum (**A** and **A'**) show specific staining in the supranuclear apical region of cells in the interlamellar region of the primary filament. No specific staining is observed in sections in which the specific primary antibody was replaced by either normal rabbit serum (**B** and **B'**), or buffer (**C** and **C'**), or in which both the primary and secondary antibodies were replaced by buffer (**D** and **D'**). Predigestion of sections with trypsin results in a high level of nonspecific fluorescence. Bar = 50 μm.

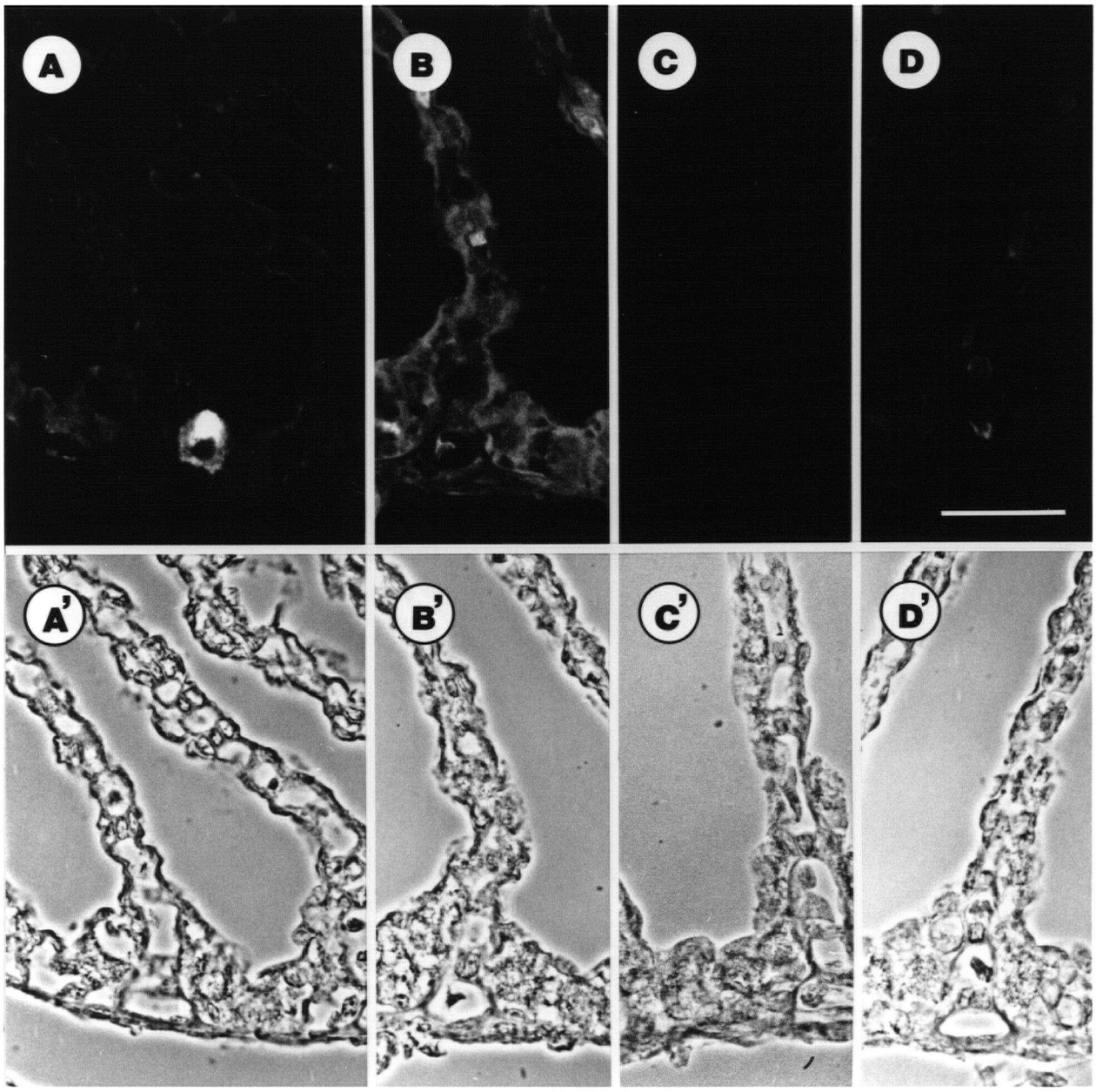
A
B
C
D
A'
B'
C'
D'

Figure 9. (**A**) Electron micrograph of mitochondrial-rich (MR) or chloride cell (CC) located in the interlamellar space of the primary filament of a dogfish gill. The nucleus is basally located and the cell has an ovoid appearance. Mitochondria can be seen along the periphery of the cell and the plasma membrane shows deep infoldings especially along its boarder with the blood space (bottom right). A dense collection of tubulovesicles (tvs) is located supranuclearly. Bar = 5 μm. The insert (**B**) shows the apically exposed surface of a MR cell. Note the subapical tubulovesicles (tvs) and apical MR-PVC (pavement cell) junctions (arrow). Bar = 0.5 μm

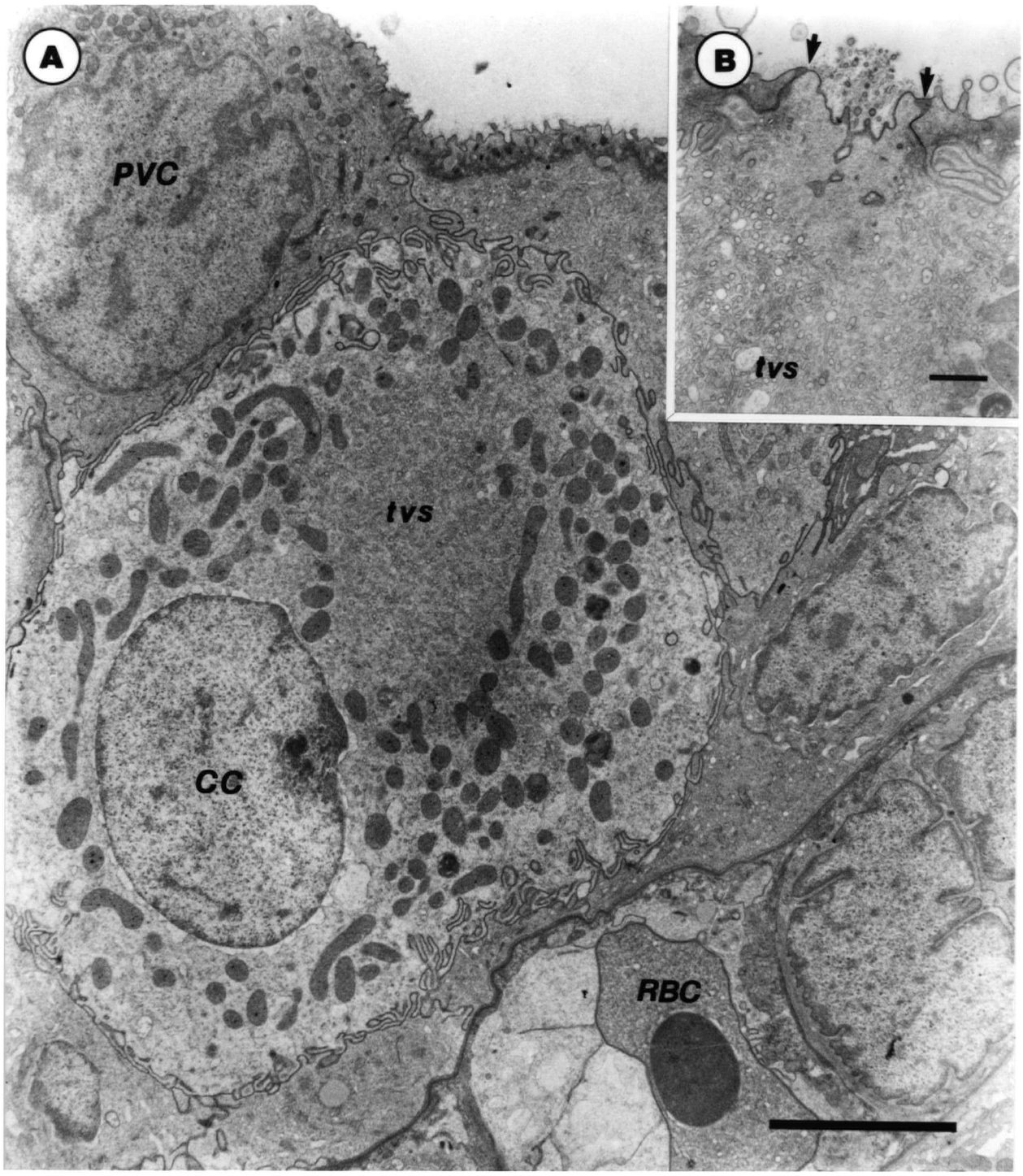
A
PVC
tvs
CC
RBC
B
tvs

Figure 10. Immunogold localization of H^+-ATPase in the gills of freshwater trout.

A.) Pavement cell (PVC) with staining associated with the apical membrane (arrow) and subapical vesicles (arrow head).

B.) Mitochondria-rich (MR) cell with a similar staining pattern as observed in PVC. A tubulovesicle is indicated with an astrisk (*). Both cells at the same magnification. Bar = 0.5 μm

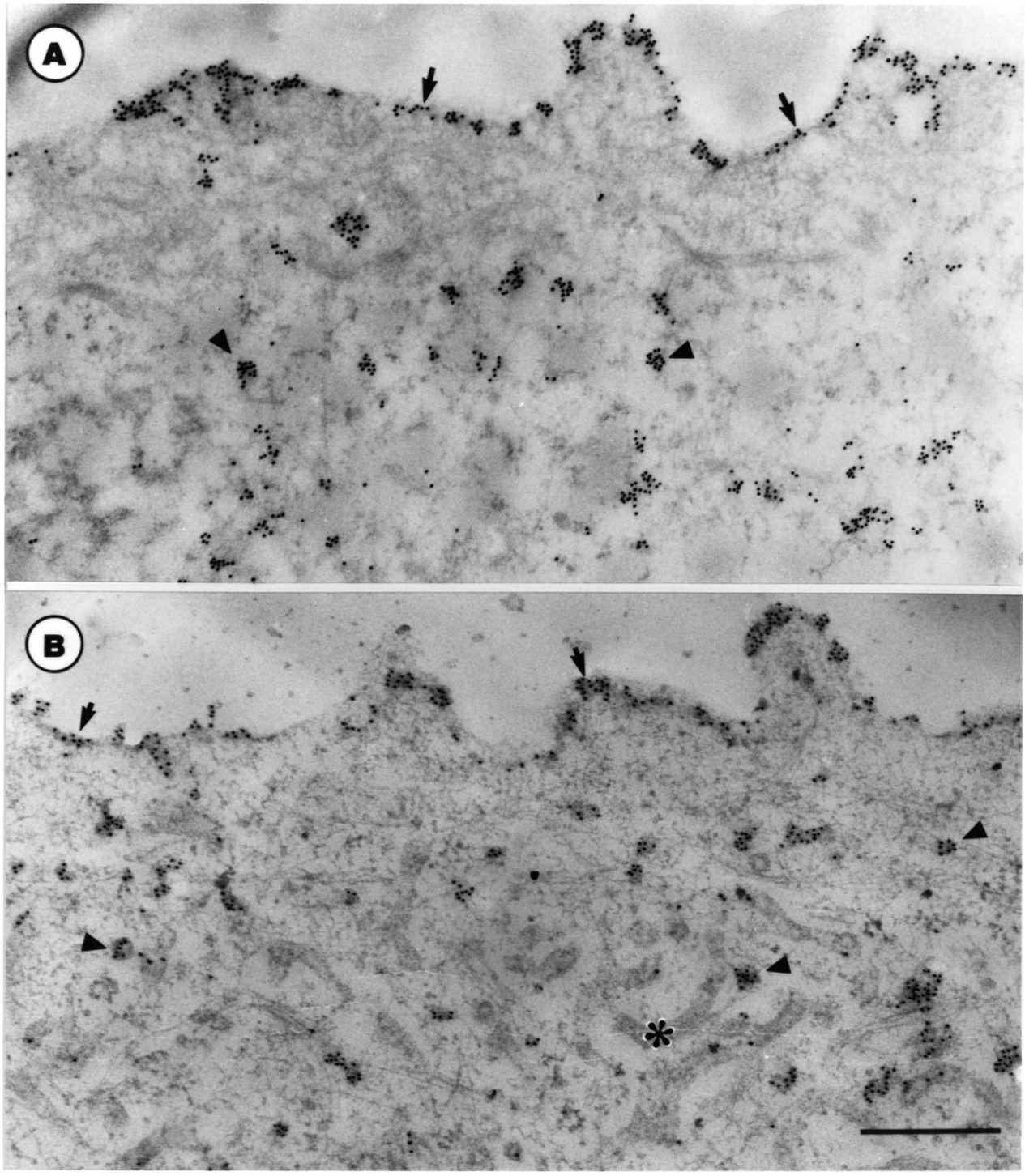
A
B

Figure 11. Western blot of dogfish gill homogenate probed with carbonic anhydrase specific polyclonal antibody. The antibodies crossreacted with the 29.5 kDa molecular weight carbonic anhydrase marker (MW), and a 30 kDa band from dogfish gill homogenate (DF). The dye front was also visible in the MW lane because pre-stained MW markers were used.

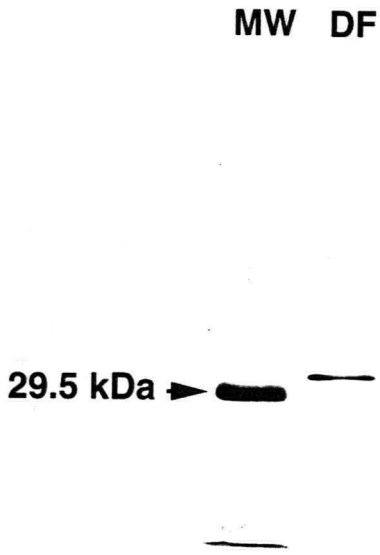
MW DF
29.5 kDa

Figure 12. Western blot of dogfish gill homogenate probed with a proton-ATPase specific polyclonal antibody. The antibodies crossreacted weakly with a band in the 70 kDa molecular weight range.


70 kDa

Table 1. Proton ATPase activity (μmol Pi · mg^{-1} Protein · h^{-1}) in *S.acanthias* crude gill homogenate at 25°C. n = 7.

ATPase Activity‡	NEM-inhibited ATPase Activity‡
0.339±0.030	**0.116±0.026***

‡ ATPase activity measured in the presence of oubain, azide, and EGTA.

* Significantly different from zero. $P<0.05$

DISCUSSION

The results from the *in situ* gill perfusion, and the *in vivo* post branchial pH change measurements suggest that CA is available to the plasma in the gills of dogfish. The general distribution of CA demonstrated in the gills of dogfish by immunocytochemistry suggests CA maybe involved in facilitation of CO_2 diffusion and /or that most of the gill epithelium may be involved in acid-base regulation. The presence of proton-ATPase in a subpopulation of MR cells in the gills, indicates directly for the first time a mechanism for acid-base /ionic regulation in elasmobranchs.

CA catalyzed plasma HCO_3^- dehydration ?

In order to assess whether or not branchial CA in elasmobranchs (Hodler *et al.* 1955) is accessible to the plasma for acceleration of HCO_3^- dehydration, an *in situ* saline perfused gill preparation was employed. The pH changes *in vivo* are complicated by a number of variables beyond the control of the experimenter (Bidani and Crandall 1988) leading to different interpretations of the data (Rispens *et al.* 1980; Chakrabarti *et al.* 1983; Hill *et al.* 1977; Crandall *et al.* 1977). The *in situ* preparation allowed me to make a clear qualitative assessment of CA availability to the plasma. The presence or absence of catalysis can be determined by measuring the pH disequilibrium state of the perfusate post-branchially because the uncatalyzed reaction is slow under physiological conditions (half time 25-90 s; Perry 1986) compared to the catalyzed reaction (beyond detection with our setup). This technique has been used by Crandall and O'Brasky (1978) to show

an acceleration of the plasma HCO_3^- dehydration reaction in the mammalian lung. The results from mammalian studies using saline perfused isolated lungs suggested that CA is available to the plasma (Crandall and O'Brasky 1978; Klocke 1978; Effros *et al.* 1978). It is now generally accepted that CA is available to the plasma in the lungs (Bidani and Crandall 1988).

During the control perfusion, the reaction was complete before the perfusate reached the post-gill electrodes suggesting that CA was available to catalyze the HCO_3^- dehydration reaction. This finding was confirmed by positive (bovine CA) and negative (ACTZ) controls. The addition of excess CA to the perfusate produced an equilibrium state and the addition of ACTZ produced a disequilibrium state as expected. The disequilibrium supposedly stemming from the inhibition of endogenous CA in the gills. This preparation clearly shows that the HCO_3^- dehydration in saline perfusing the gills is being accelerated.

Other sources of CA activity in the preparation may come from trapped or lysed erythrocytes. Flushing the preparation for 10 to 20 min at a rate of 1.5 $l \cdot h^{-1}$ resulted in complete blanching of the gills. This macroscopic observation of the gills suggests that there were no erythrocytes remaining. The contents of lysed erythrocytes are also likely washed away by this process. Henry *et al.* (1986) suggested that the source of plasma available pulmonary CA in mammals may be from lyzed erythrocytes but the finding of *de novo* CA synthesis in cultured endothelial cells is contradictory (Ryan *et al.* 1982). Membrane associated CA is thought to be held in place by a phosphatidylinositol-glycan (PI-G) anchor (Low *et al.* 1988).

The distribution of CA demonstrated by immunofluorescence lacks the detailed cellular information necessary for determining if CA is associated with the blood side of the pillar cell membrane (Figure 6). Immunocytochemical and less convincingly histochemical (Hansson 1967) localization techniques for CA employed at the EM level have been used to determine CA accessibility to the plasma in respiratory epithelia (Ryan *et al.* 1982; Rahim *et al.* 1988; and Lönnerholm 1982, respectively). The histochemical results are not as convincing because the reaction product (cobalt precipitate) is deposited diffusely around the reaction locus (site of the enzyme). Therefore, it is not possible to say for certain which side of the membrane the reaction originates (Lönnerholm 1982). The information about pillar cell membrane associated CA was to be provided by immunoelectron microscopy but unfortunately those experiments were not successful. One possibility for the lack of success with immunogold technique is that the alcohol dehydration of the tissue (necessary for infiltration of embedding media) interferes with the antigenicity of the protein.

Apart from the limitations of the immunofluorescence technique with respect to a membrane associated CA, there is also the possibility that the avian CA II polyclonal antibody did not crossreact with the membrane-associated isozyme (CA IV). Whitney and Briggle (1982) have characterized a membrane associated CA isozyme (CA IV) from bovine lung. This isozyme has an apparent molecular weight of 52 kDa, 20% of which is accountable by carbohydrate. The CA IV has half the specific activity of the erythrocytic CA isozyme, sensitivity to ACTZ (K_i = 10 nM), and insensitivity to inhibition by antiserum to erythrocyte CA. Wistrand and Knuuttila (1989) have also purified and

characterized a membrane associated enzyme (CA IV) from human renal membranes with an apparent molecular weight of 35 kDa. The CA IV peptide is not any longer than the cytosolic CA isozymes (~30 kDa). The higher apparent molecular weight is a consequence of the carbohydrate portion. Western blot analysis of elasmobranch gill homogenates (Figure 11) confirmed the specificity of the polyclonal antibodies for the 30 kDa CA (Bergenhem *et al.* 1986) but what was not shown was a crossreactive higher molecular weight band. Maynard and Coleman (1971) have reported higher (36-39 kDa) molecular weight CA isozymes in tiger (*Galeocerdo cuvieri*) and bull (*Carcharhinus leucas*) shark erythrocytes under non-reducing conditions (native protein). However, Bergenhem *et al.* (1986) later showed that glutathione and cysteine, coupled via disulphide linkages, accounted partially for the higher reported molecular weight rather than a longer polypeptide. The lack of detection by Western blot analysis of a CA IV suggests that the immunofluorescene may not be accounting for all the CA in the gills because of a lack of probe crossreactivity with the CA IV isozyme.

A similar finding was made by Lönnerholm and Wistrand (1984) who found that localization of CA in kidney with a probe raised against CA II (HCA C) could not account for all the CA activity shown by another method (Hansson's method). The Hansson's (1967) histochemical method localizes sites of active CA catalysis on a section irrespective of isozyme types. The localization of CA by Brown *et al.* (1990) in rat kidney using antibodies raised against purified CA IV and CA II accounted for all the histochemical CA distribution reported by Lönnerholm and Wistrand (1984). Thus the distribution of CA in dogfish gill may be more extensive than observed because only

isozyme(s) crossreactive with CA II probe were determined. There may also be CA IV activity as in mammalian kidney and lung.

The *in vivo* pH change with ACTZ treatment (Figure 3a) and stopped-flow pH changes (Figure 3b) are consistent with the hypothesis that branchial CA activity is available to the plasma. When compared with observations from similar studies in teleost fish (Henry *et al.* 1988, 1995; Gilmour *et al.* 1994), in which CA is known to be unavailable to the plasma (Perry *et al.* 1982, Rahim *et al.* 1988, Henry *et al.* 1988), the elasmobranch appears to have a different distribution of branchial CA.

The administration of ACTZ is associated with an acidosis in both dogfish (this study) and trout (Henry *et al.* 1988, 1995). The rate of the onset of the acidosis can be related to the location or availability of the CA since ACTZ diffuses relatively slowly through the erythrocyte membrane (K_{in} 21-27 h^{-1}; Holder and Hayes 1965) (>5min for 50% rbc CA inhibiton in dogs; Effros *et al.* 1980). An immediate pH change may reflect inhibition of directly available CA (plasma accessible). In teleosts in which CA has been found to be unavailable to the plasma, the onset of the acidosis after ACTZ administration is delayed (10-20 min; Henry *et al.* 1988) compared to that observed for dogfish. The teleost acidosis is correlated with erythrocyte CA inhibition.

The recovery from acidosis in dogfish was within 40 min of ACTZ infusion. Since the post-branchial pH disequilibrium remained unchanged, it is unlikely that an increase in CA activity or a decrease in inhibition are responsible. Compensatory mechanism(s) operating independently of CA are likely recruited to correct the drop in pH. Swenson and Maren (1986) demonstrated that the elasmobranch kidney can excrete

acid using mechanisms independent of CA or CO_2. However, Henry *et al.* (1988) did not observe a recovery from ACTZ treatment after 24 h in channel catfish. The difference in findings may be related to the dependence of teleost compensatory mechanisms on CA (Nishimura 1977) and the difference in the total amount of inhibitor added per fish. Our concentration of 10^{-4} M was based on a final volume one quarter of the volume used by Henry *et al.* (1988) (5% body weight, blood volume, versus ~20% body weight, extracellular fluid volume, respectively).

The *in vivo* post-branchial pH drop observed in the extracorporeal loop using the stopped-flow technique in dogfish provides indirect evidence for branchial CA activity available for plasma CO_2 reactions. The stopped flow pH changes in post-branchial blood represent a correction of the disequilibrium between blood compartments created during CO_2 elimination. The interpretation of our data is based on predictions from mammalian models in which pulmonary CA activity has been demonstrated (Bidani and Crandall, 1978, Effros *et al.* 1978, Hill *et al.* 1977). Mathematical models have allowed predictions of post-pulmonary, or in our case post-branchial, pH changes under a variety of theoretical conditions (e.g. Crandall and Bidani 1981; Zock *et al.* 1981). Similarities in our results with the predictions by Crandall and Bidani (1981) help to explain our observations. Crandall and Bidani (1981) predicted a post capillary pH *decrease* in plasma exposed to high levels of CA ($A_o > 100$; A_o extracellular pulmonary catalysis factor, catalyzed: uncatalyzed rate) during lung transit, the magnitude being inversely proportional to the erythrocyte HCO_3^- permeability (P_{HCO3-}) or Cl^- / HCO_3^- exchange. At $A_o = 1$ or no extracellular CA activity, a small post pulmonary pH *increase* would be

predicted by the model even with impaired P_{HCO3}. These predictions were confirmed by observed pH changes in *in vitro* blood perfused rat lungs (Crandall *et al.* 1981). Crandall *et al.* (1981) inhibited Cl^- / HCO_3^- exchange by pretreatment of erythrocytes with DIDS (4,4'-diisothiocyanostilbene-2,2'disulphonic acid; a potent anion exchange inhibitor) and showed a pronounced pH decrease in the post-pulmonary perfusate whereas the perfusion with untreated erythrocytes was not associated with a measurable disequilibrium. The post-pulmonary pH decrease results because the catalyzed rate of dehydration made possible by endothelial CA and the relatively poor buffering capacity of plasma compared to erythrocytes result in a large, rapid fall in plasma $[H^+]$. After leaving the lungs the disequilibrium between blood compartments is corrected by the Jacobs-Stewart cycle by which H^+ ions are transferred from the erythrocyte to the plasma via CO_2 (Figure 13) . Conversely, if thought of in terms of a HCO_3^- disequilibrium then a limitation of Cl^- / HCO_3^- exchange during gill transit would result in continued Cl^- / HCO_3^- exchange post-branchially and the same associated increase in plasma $[H^+]$ via the Jacobs-Stewart cycle.

If the predictions of Crandall and Bidani (1981) are applied to the *in vivo* situation in dogfish, then high branchial CA activity available to the plasma would not be expected to be associated with an equilibrium situation but the infusion of exogenous CA resulted in a rapid equilibration of blood prior to stopped-flow measurements. The discrepancy is clarified when the availability of CA to different parts of the system (i.e. branchial restricted CA activity versus CA activity available branchially and post-branchially in the stopped flow electrode chamber) is considered. In the former, the

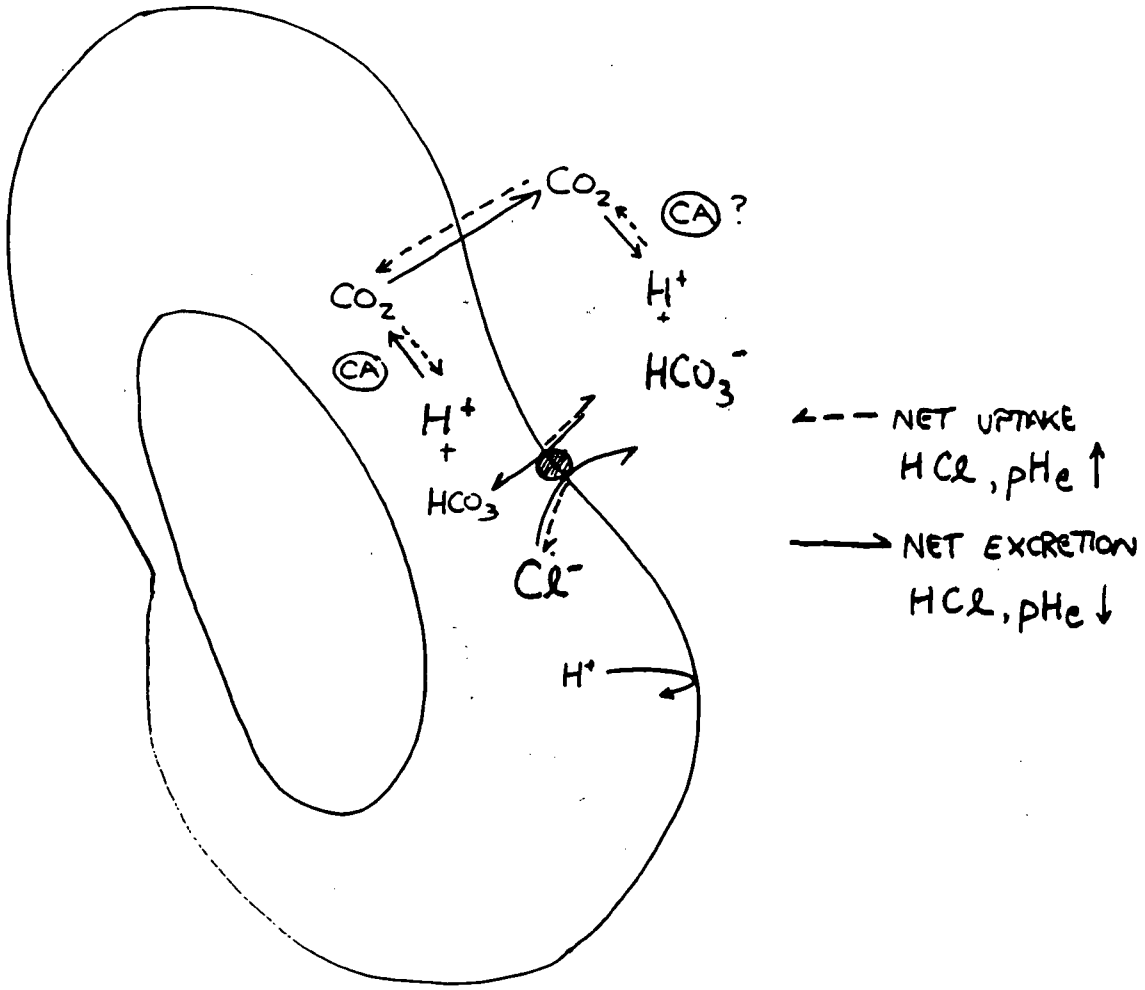

Figure 13. Illustration of the correction of disequilibria between the blood compartments, erythrocyte (RBC) and plasma, via the Jacobs-Stewart cycle.

disequilibrium created during gill transit is corrected slowly post-branchially, but in the latter the correction is very rapid (catalyzed by exogenous CA). The 6 s delay before the stopped flow measurement may be sufficient for the equilibration to be completed. Therefore, if CA is traveling in the plasma, any disequilibrium created during CO_2 elimination in the lungs/ gills will be rapidly corrected by CA before the stopped-flow measurement. In addition, our results indicate that the endogenous plasma CA activity reported in separated plasma of *Scyliorhinus canicula* by Wood *et al.* (1994) is insufficient to obliterate the post branchial pH disequilibria as seen during the infusion of exogenous CA. It follows that CA infusion is an inappropriate control in this series of experiments. Under these conditions it cannot be determined if Cl^- / HCO_3^- exchange would be the rate limiting step in CO_2 elimination as suggested by Gilmour *et al.* (1994) using this control. The argument is that in the presence of an excess of CA activity in the intra and extracellular blood compartments, Cl^- / HCO_3^- exchange will be the rate limiting step (Figure 13). It is unknown whether the Cl^- / HCO_3^- exchanger is rate limiting under resting conditions in elasmobranchs (Obaid *et al.* 1979; Payne and Evans 1988) but the control period pH change indicates the rate limitation of erythrocyte Cl^-/ HCO_3^- exchange may contribute to the HCO_3^- disequilibrium.

The model predicted a negative post-pulmonary pH disequilibrium when the plasma reaction during gill transit was catalyzed. In the absence of branchial CA activity available to the plasma such as in the trout (Gilmour *et al.* 1994; Rahim *et al.* 1988; Henry *et al.* 1988) or when branchial CA is inhibited, HCO_3^- dehydration would be dependent on erythrocyte CA. But in the presence of extracellular branchial or pulmonary

CA activity HCO_3^- dehydration need not be dependent on erythrocyte CA. In the dogfish the dependence on erythrocyte CA is further diminished because of the lower intracellular CA activity (1/12 of teleost, Maren *et al.* 1980), and the lack of a Haldane effect (Tufts and Randall 1989; Jensen 1989; Wood *et al.* 1994).

The post-branchial pH *increase* observed during inhibition of CA with ACTZ probably resulted from the slow uncatalyzed plasma HCO_3^- dehydration. The magnitude of the pH disequilibium remained unchanged after 60 min inhibition. The lack of change in the magnitude would suggest that the post branchial pH change is independent of the degree of erythrocyte inhibition. CA is generally considered to be present in excessive amounts within the erythrocyte (Swenson, 1990). In contrast to the pH increase seen in elasmobranchs, the ACTZ treatment in trout results in an acidotic disequilibrium, pH decrease (Gilmour *et al.* 1994). The prominent Haldane effect (oxygenation of Hb causes release of Bohr protons) in trout (Jensen 1989) leads to a shift of intracellular protons to the plasma via the Jacobs-Stewart cycle as the blood flows away from the gills. The Haldane effect is functionally absent in elasmobranch blood.

The contribution of branchial plasma available CA to CO_2 elimination in dogfish is unclear. For humans, Crandall and Bidani (1981) estimated lung CA maximally accounts for < 10% of CO_2 elimination. Much of the information on elasmobranchs has been collected using differential inhibition of CA. The specificity of CA inhibitors is based partly on their membrane permeability. Polymer inhibitors are restricted to the extracellular space by virtue of their size, inhibiting extracellular CA specifically. Benzolamide is relatively impermeable to erythrocytes compared to branchial cells

resulting in 40% and 98% CA inhibition, respectively, and methazolamide is not cell type specific at all (99% erythrocyte and 99% branchial CA inhibition) (Swenson and Maren 1987). Unfortunately there is no inhibitor specific for erythrocyte CA. Swenson and Maren (1987) reported that inhibition of branchial CA in resting fish with benzolamide (gill) had no effect on blood acid-base parameters (pH, P_{CO2}, $[HCO_3^-]$) except for a slight rise in $[HCO_3^-]$ (0.7 mM) while inhibition with methazolamide (both erythrocyte and gill) resulted in a transient acidosis accompanied by increasing P_{CO2}, and $[HCO_3^-]$. These results suggest CO_2 gradients and hence CO_2 elimination can be maintained without branchial CA. However, the repeated finding of Swenson *et al.* (1982, 1984; Swenson and Maren 1987) that inhibition of branchial CA with benzolamide (gill specific) results in a decreased ability to eliminate a HCO_3^- load (9 mEq $\cdot$ kg^{-1}) suggests that plasma accessible branchial CA catalyzes the dehydration of HCO_3^- to CO_2 which is easily eliminated by diffusion. More recently, Swenson *et al.* (1995) have demonstrated that specific inhibition of plasma accessible branchial CA with a plasma restricted polymer inhibitor produces the same result. It would appear that the importance of branchial CA in relieving the base load may be related to a limitation in erythrocyte Cl^- / HCO_3^- exchange making erythrocyte CA less accessible. There is little evidence in elasmobranchs correlating CO_2 elimination with haematocrit (Hct) which would give an indication of the physiological dependence of HCO_3^- dehydration on erythrocytic CA. However, Evans *et al.* (1984) demonstrated perfusion of head preparations with a washed erythrocyte suspension (Hct 8%) resulted in a greater CO_2 excretion compared with a saline perfusion.

Another potential cause for the pH disequilibrium could be the mixing of arterial and shunted venous blood post-branchially (Klocke 1980). There is no anatomical evidence for a direct connection between the ventral and dorsal aorta bypassing the lamellae (Olson and Kent 1980; Metcalfe and Butler 1986). De Vries and De Jager (1984) showed that 4% of the basal lamellae are covered by a branchial canopy (a sheet of tissue from the gill arch) in *S. acanthias* but this does not appear to represent a ventilatory dead space as in the Endeavour dogfish (*Centrophorus scalpratus*; Cooke 1980). The canopy prevents ventilatory water from flowing over the lamellae creating a shunt for venous blood. Shunting, however, can also be achieved by altering the ventilation perfusion ratio (Piiper and Scheid 1984). In the closed system of the post-branchial stopped-flow chamber, the acidotic disequilibrium probably resulted from the HCO_3^- movement into the erythrocyte driving the Jacobs-Stewart cycle (acidification of the plasma). The initial HCO_3^- disequilibrium is the result of either a limitation in Cl^- / HCO_3^- exchange in the presence of plasma accessible CA during gill transit (discussed earlier) or the addition of venous blood which has a higher [HCO_3^-] than arterial blood. It is not possible to distinguish between these possibilities at this time.

Branchial cytosolic carbonic anhydrase

Immunolocalization of CA with an avian CA II polyclonal antibody revealed a general distribution throughout the branchial epithelium (Figure 5 and 6). The specificity of the antibody was verified by Western blot analysis (Figure 11) and the use of appropriate incubation controls (Figure 6b-d). The diffuse cytoplasmic staining of

epithelial cells suggests that CA may be involved in providing intracellular counter ions for acid-base / ion regulation or possibly to facilitate diffusion of CO_2 across the epithelium.

A comparison of our immunolocalization with the histochemical Hansson's method used by Conley and Mallatt (1987) on the leopard shark (*Triakis semifasciatus*) revealed quite different results. They found CA activity localized to the gill MR cells and erythrocytes and not to lamellar pavement cells or pillar cells. The lack of correlation with the two techniques is more likely representative of a species difference than a difference in technique. After analyzing seventeen species of fish, Conley and Mallatt (1987) concluded that there was a large interspecific variation in the distribution pattern of CA. Also the species with similar patterns of distribution did not show a correlation with environment or lifestyle. It would be interesting to see whether or not the MR cells with CA activity in *T. semifasciatus* also label positive for H^+-ATPase.

It has also been demonstrated that CA can facilitate CO_2 elimination when CO_2 diffusion is rate limiting (Enns and Hill 1983; Heming *et al.* 1986). CO_2 diffusion is enhanced or facilitated by the codiffusion of HCO_3^- and buffered H^+. The degree of codiffusion is determined by the buffer quantity and mobility, the pH, the absolute P_{CO2}, and P_{CO2} gradients (eg. Gros *et al.* 1976; Gros 1991). Schultz (1980) demonstrated in artificial membranes that facilitation of CO_2 diffusion would be optimal when CA was distributed homogeneously across the path of diffusion. This spatial distribution is seen in the gill epithelium of dogfish (Figures 5 and 6). However, it is unclear as to whether the distribution of CA is reflective of a need for facilitated diffusion since CO_2 diffusion is

not rate limiting under physiological conditions (review Perry 1986; Butler and Metcalfe 1988; Swenson 1990).

The gills of elasmobranch fishes have been clearly established as the predominant site of acid-base relevant ion transfer with less than 3% of the net acid excretion being accounted for by extra-branchial routes (kidney, abdominal pore, rectal gland) under a variety of acidotic conditions (summary Heisler 1988). Branchial cytosolic CA hydration of CO_2 provides H^+ and HCO_3^- for acid-base regulation.

The accumulated evidence, albeit indirect, suggests that acid excretion in the gills of elasmobranchs is coupled to Na^+ uptake but does not define the precise nature of the exchange (reviews Heisler 1988; Shuttleworth 1988; Evans 1993). Na^+ influx has been shown to be sensitive to changes in water (Bentley *et al.* 1976) and blood (Payan and Maetz 1973) pH as well as to ACTZ (Payan and Maetz 1973). H^+ efflux has been shown to be sensitive to changes in water [Na^+] (Bentley *et al.* 1976; Evans 1982; Evans *et al.* 1979) and external amiloride (10^{-4} M; Evans *et al.* 1979). The disadvantage of the Na^+ / H^+ antiporter mechanism is that during an acidosis when H^+ efflux is increased an increased salt load will result. Heisler (1988) calculated that during environmental hypercapnia or severe lactacidosis (H^+ equivalent efflux > 15 $\mu mol \cdot kg^{-1}$ bw $\cdot$ min^{-1}; *Scyliorhinus stellaris*) the ionic load would be roughly doubled if ions are equivalently transferred. The ionic load is probably excreted via the rectal gland (8.3 - 12.5 $\mu mol \cdot kg^{-1}$ bw $\cdot$ min^{-1}; *S. acanthias*; Shuttleworth 1988) since the gills are the site of net salt influx (review Shuttleworth 1988). In contrast to the gills, the mechanisms for ion (NaCl) excretion in the rectal gland have been well characterized (Riordan *et al.* 1994).

It is not known whether the Na^+ / H^+ exchange is driven by a proton ATPase in seawater fish as has been shown in freshwater teleost fish (Lin and Randall 1995). The Na^+ / H^+ antiporter is favourable since the inward Na^+ gradient is sufficient to drive acid excretion. However, the lack of complete inhibition (50%) of H^+ efflux by amiloride (10^{-4} M, Evans *et al.* 1979) suggests that other mechanism(s) besides a Na^+ / H^+ antiporter are involved (Dale 1982). Indeed, H^+-ATPase activity (Lin and Randall 1993) and distribution (Lin *et al.* 1994) are reduced after seawater acclimation of teleosts. The low levels of enzyme activity in crude homogenates (Table 1) and limited distribution in the epithelium (Figure 6 and 7) taken together with the information on the distribution of CA (Figure 4 and 5) suggest that H^+-ATPase has a restricted distribution in the gills of elasmobranchs and is unlikely to be the major mechanism for acid-base regulation.

The pretreatment of sections with trypsin was required to enhance reactivity of dogfish H^+-ATPase with rabbit antiserum to bovine 70 kDa subunit of H^+-ATPase. In the conventional preparations for immunofluorescence microscopy the antibody did not show cross reactivity. Trypsin treatment of sections is believed to etch the surface of sections thereby 'unmasking' epitopes (Curran and Gregory 1977). The specificity of the H^+-ATPase antibody was verified by Western blot analysis (Figure 12) and the use of appropriate incubation controls (Figure 5b-d; for additional information see Lin *et al.* 1994 and Südhof *et al.* 1989).

It is possible that H^+ excretion is shared by the two mechanisms as shown in different segments of the mammalian kidney (review Gluck and Nelson 1992). In the proximal tubule, and thick ascending limb, apical plasma membrane proton ATPase

accounts for 33%, and 20%, respectively, of the H^+ secretion while a Na^+ / H^+ antiporter accounts for the rest (Gluck and Nelson 1992).

It is unlikely that ammonia excretion is used as a mechanism for acid-base regulation (review Heisler 1988). Ammonia has been shown to be eliminated predominantly by non-ionic diffusion (~75%) and the remainder by ionic NH_4^+ diffusion (Evans 1985). However, in *S. acanthias* ammonia excretion has been reported to increase during hypercapnia (Claiborne and Evans 1985) but this maybe secondary to acid excretion (NH_3 with H^+ rather than NH_4^+).

H^+-ATPase indirectly coupled to a Na^+ channel is not as an attractive proposition for a seawater fish as it is for its freshwater counterpart. Electroneutrality is maintained but osmotically active particles (Na^+) are also accumulated. We can speculate that the pmf (proton motive force) generated by the proton ATPase could drive Cl^- efflux via an apical Cl^- channel but this prospect is unlikely since Cl^- efflux has been shown to be unaffected by changes in water pH (Bentley *et al.*, 1976). The pH change (pH 7.8 to 6.9) was, however, still within the reported operating range of the freshwater trout proton pump (pH 5.5- 8; Lin and Randall 1991).

The operation of a H^+-ATPase maybe exclusively for acid-base regulation as in some other epithelia (e.g. mammalian kidney collecting duct, Verlander *et al.* 1988; Alper *et al.* 1989). Mitochondria-rich (MR) cells are a characteristic feature of acid-base regulatory epithelia (toad skin, Larsen 1991; turtle bladder, Steinmetz 1986; mammalian collecting duct, Alper *et al.* 1989). These MR cells are associated with high intracellular CA activity, and a heavily invaginated basolateral membrane. The polarity of the cell is

determined by the distribution of acid and base translocating mechanisms: an electrogenic H^+-ATPase and an electroneutral Cl^-/ HCO_3^- antiporter. The acid excreting α-type MR cell has an apical H^+-ATPase and a basolateral Cl^- / HCO_3^- exchanger. The base excreting β-type MR cell has an apical Cl^- / HCO_3^- exchanger and basolateral H^+-ATPase.

The staining pattern of the dogfish MR cells is reminiscent of α-type cells (Brown *et al.* 1987b, 1988). The intense granular labeling with the H^+-ATPase antibodies associated with the tubulovesiclar system suggests that a portion of the pumping capacity may be placed in reserve (review Brown 1989; Gluck *et al.* 1992). Potentially during an acidosis when the need for active pumping units is required, these vesicles are recruited and inserted into the apical membrane (Schwartz and Al-Awqati 1985; Brown *et al.* 1987b). In rat kidney α-type cells (Brown *et al.* 1987a) and bullhead catfish gill pavement cells (Laurent *et al.* 1994) the H^+-ATPase vesicles have been characterized as non-clathrin coated.

In summarizing the CA and H^+-ATPase distributions in gills of spiny dogfish, *S. acanthias*, it would be interesting to make a comparison with the fresh and seawater adapted rainbow trout, *O. mykiss*. The differences between the two species may reflect the adaptations in gill function between these two distantly related species. The distributions of CA and H^+-ATPase demonstrated by Rahim *et al.* (1988) and Lin *et al.* (1994), respectively, in freshwater trout show a remarkably similar distribution. The CA catalyzed hydration of CO_2 intracellularly provides counter ions for acid-base or ion regulation. The apical distribution of CA in the outer epithelium is probably related to its

role in providing H^+ for the electrogenic proton pump. The electrochemical gradient created across the apical membrane can drive Na^+ uptake via a channel (e.g. Harvey 1992) and possibly Cl^- uptake via a Cl^- / HCO_3^- exchanger (γ type cell) (Riestenpatt *et al.* 1995; Larsen 1991; Larsen *et al.* 1992)(Potts 1994). The presence of H^+-ATPase has been demonstrated along the apical membrane of both freshwater MR cells and pavement (PVC) cells (Figure 10). Evidence from Goss *et al.* (review Goss *et al.* 1995) and Morgan *et al.* (1994) suggests that Cl^- uptake is via the MR cell and that Na^+ uptake is via the PVC. In the seawater adapted trout the H^+-ATPase distribution is reduced (Lin *et al.* 1994) but the concentration of CA increased but with the same distribution pattern (Perry and Laurent 1990). The CA in trout may also be effective in facilitating CO_2 diffusion across the epithelia (Schultz 1980) but it is not associated with the catalyzed plasma HCO_3^- dehydration reaction (Perry *et al.* 1982; Rahim *et al.* 1988; Henry *et al.* 1988). In addition, the presence of endogenous CA inhibitor in the plasma of trout (Haswell and Randall, 1976; and some mammals, Rispens *et al.* 1985) suggests that CA presence in the plasma may have detrimental effects on some aspect of the animal's physiology. Nikinmaa *et al.* (1990) showed that addition of CA to trout plasma *in vitro* would short circuit β-adrenergic stimulated pH regulation (Na^+-H^+ exchange) of the red blood cell. Lessard *et al.* (1995), however, found no *in vivo* effect. It has yet to be substantiated whether the absence of red blood cell β-adrenergic stimulated Na^+-H^+ exchange in dogfish (Tufts and Randall 1989) is related to the presence of plasma CA activity (Wood *et al.* 1994). To recap, the trout has a CA distribution suited for subserving ion / acid-base exchange mechanisms (e.g. H^+-ATPase), and possible facilitated diffusion of CO_2 while

the general CA distribution in dogfish seems particularly well suited for facilitated diffusion of CO_2 and potentially acid-base regulation (Na^+/ H^+, Cl^- / HCO_3^- exchange). In addition, dogfish branchial CA has the capacity to catalyze the plasma HCO_3^- dehydration reaction. The observations by Conely and Mallat (1987) would not allow us to extend our observations of *S. acanthias* to all elasmobranchs.

CONCLUSIONS:

1.) The *in situ* gill perfusion study demonstrates that CA activity associated with pillar cell membrane is available to catalyze HCO_3^- dehydration in the plasma.

2.) The *in vivo* observations provide equivocal evidence for the availability of CA to the plasma.

3.) The general immunolocalization of CA in the gills suggests the involvement of most of the epithelium in acid-base regulation and/or facilitated diffusion.

4.) The immunolocalization of H^+-ATPase in some MR cells in the gills (Figures 7 and 8), and measurable NEM sensitive ATPase activity in gill homogenates indicates directly for the first time a mechanism for acid-base or ionic regulation in elasmobranchs.

REFERENCES

Alper, S.L., J. Natale, S. Gluck, H.F. Lodish, and D. Brown (1989). Subtypes of intercalated cells in rat kidney collecting duct defined by antibodies against erythroid band 3 and renal vacuolar H^+-ATPase. Proc. Natl. Acad. Sci. USA *86*:5429-5433.

Bentley, P.J., J. Maetz, and P. Payan (1976). A study of the unidirectional fluxes of Na and Cl across the gills of the dogfish *Scyliorhinus canicula* (Chondrichthyes). J. exp. Biol. *64*:629-637.

Bergenhem, N., U. Carlsson, and L. Strid (1986). The existence of glutathione and cysteine disulfide-linked to erythrocyte carbonic anhydrase from tiger shark. Biochim. Biophys. Acta *871*:55-60.

Bidani, A., and E.D. Crandall (1988). Velocity of CO_2 exchanges in the lungs. Ann. Rev. Physiol. *50*:639-652.

Bjerrum, O.J. and C. Schafer-Nielsen (1986). In: Analytical Electrophoresis. M.J. Dunn, ed. Verlag Chemie, Weinheim. pp. 315

Blake, M.S., K.H. Johnston, G.J. Russell-Jones, and E.C. Gotschlich (1984). A rapid, sensitive method for detection of alkaline phosphatase-conjugated anti-antibody on western blots. Anal. Biochem. *136*:175-179.

Blattler, D.P., F. Garner, K. van Slyke, and A. Bradley (1972). Quantitative electrophoresis in polyacrylamide gels of 2-40%. J. Chromatography *64*:147-155

Bradford, M.M. (1976). A rapid and sensitive method for the quantitation of microgram quantities of protein utilizing the principle of protein-dye binding. Anal. Biochem. *72*:248-254.

Brown, D. (1989). Membrane recycling and epithelial cell function. Am. J. Physiol. *256*:F1-F12.

Brown, D., S. Gluck, and Hartwig (1987a). Structure of the novel membrane-coating material in proton-secreting epithelial cells and identifcation as an H^+-ATPase. J. Cell Biol. *105*:1637-1648.

Brown, D., P. Weyer, and L. Orci (1987b). Nonclathrin-coated vesicles are involved in endocytosis in kidney collecting duct intercalated cells. Anat. Rec. *218*:237-242.

Brown, D., S. Hirsch, and S. Gluck (1988). Localization of a proton-pumping ATPase in rat kidney. J. Clin. Invest. *82*:2114-2126.

Brown, D., X.L. Zhu, and W.S. Sly (1990). Localization of membrane-associated carbonic anhydrase type IV in kidney epithelial cells. Proc. Natl. Acad. Sci. USA *87*:7457-7461.

Butler, P.J., and J.D. Metcalfe (1988) Cardiovascular and respiratory systems. In: Physiology of the Elasmobranch Fishes. T.J. Shuttleworth, ed. Springer-Verlag, Berlin, pp. 1-39.

Chakrabarti, M.K., S.M. Cobbe, L. Loh, and P.A. Poole-Wilson (1983). Measurement of pulmonary venous and arterial pH oscillations in dogs using catheter tip pH electrodes. J. Physiol. *336*:61-71.

Claiborne, J.B., and D.H. Evans (1985). Acid-base balance in the spiny dogfish (*Squalus acanthias*) during hypercapnia. Bull. Mt. Desert Isl. Biol. Lab. *25*:28-30.

Conley, D.M., and J. Mallatt (1987). Histochemical localization of Na^+-K^+ ATPase and carbonic anhydrase activity in gills of 17 fish species. Can. J. Zool. *66*:2398-2405.

Cooke, I.R.C. (1980). Functional aspects of the morphology and vascular anatomy of the gills of the endevour dogfish, *Centrophorus scalpratus* (McCulloch) (Elasmobranchii: Squalidae). Zoomorph. *94*:167-183.

Crandall, E.D., A. Bidani, and R.E. Forster (1977). Postcapillary changes in blood pH in vivo during carbonic anhydrase inhibition. J.Appl.Physiol. *43*:582-590.

Crandall, E.D., and A. Bidani (1981). Effects of red blood cell HCO_3^-/Cl^- excchange kinetics on lung CO_2 transfer: theory. J.Appl.Physiol. *50*:265-271.

Crandall, E.D., and J.E. O'Brasky (1978). Direct evidence for participation of rat lung carbonic anhydrase in CO_2 reactions. J. Clin. Invest. *62*:618-622.

Crandall, E.D., S.J. Mathew, R.S. Fleischer, H.I. Winter, and A. Bidani (1981). Effects of inhibition of RBC HCO_3^-/Cl^- exchange on CO_2 excretion and downstream pH disequilibrium in isolated rat lungs. J. Clin. Invest. *68*:853-862.

Curran, R.C., and J. Gregory (1977). The unmasking of antigens in paraffin sections of tissue by trypsin. Experientia *33*:1400-1401.

Dale, B. (1982). Amiloride: a molecular probe of sodium transport in tissue and cells. Am. J. Physiol. *242*:C131-C145.

De Vries, R., and S. De Jager (1984). The gill in the spiny dogfish, *Squalus acanthias*: respiratory and nonrespiratory function. Am. J. Anat. *169*:1-29.

Dimberg, K., B. Hoglund, P.G. Knutsson, and Y. Ridderstrale (1981). Histochemical localization of carbonic anhydrase in gill lamellae from young salmon (*Salmo salar* L.) adapted to fresh and salt water. Acta Physiol. Scand. *112*:218-220.

Effros, R.M., R.S.Y. Chang, and P. Silverman (1978). Acceleration of plasma bicarbonate conversion to carbon dioxide by pulmonary carbonic anhydrase. Science *199*:427-429.

Effros, R.M., L. Shapiro, P. Silverman, and M. Lieber (1980) Pulmonary capillary carbonic anhydrase. In: Biophysics and Physiology of Carbon Dioxide. C. Bauer, G. Gros, and H. Bartels, eds. Springer-Verlag, Berlin, pp. 339-342.

Enns, T., and E.P. Hill (1983). CO_2 diffusing capacity in isolated dog lung lobes and the role of carbonic anhydrase. J.Appl.Physiol. *54*:483-490.

Evans, D.H. (1982). Mechanisms of acid extrusion by two marine fishes: the teleost, *Opsanus beta*, and the elasmobranch, *Squalus acathias. J. exp. Biol. 97:289-299.*

Evans, D.H. (1985) Modes of ammonia transport across fish gills. In: Transport Processes, Iono- And Osmoregulation. R. Gilles, and M. Gilles-Baillien, eds. Springer-Verlag, Berlin, pp. 169-176.

Evans, D.H. (1993) Osmotic and ionic regulation. In: The Physiology of Fishes. D.H. Evans, ed. CRC Press, Inc, Boca Raton, pp. 315-341.

Evans, D.H., G.A. Kormanik, and E.J. Krasny JR (1979). Mechanisms of ammonia and acid extrusion by the little skate, *Raja erinacea*. J. exp. Zool. *208*:431-437.

Evans, D.H., J.B. Claiborne, and S.D. Robbins (1984). Erythrocytes play a significant role in CO_2 excretion across the shark gill. Bull. Mt. Desert Isl. Biol. Lab. *24*:22-23.

Forster, R.P., L. Goldstein, and J.K. Rosen (1972). Intrarenal control of urea reabsorption by renal tubules of the marine elasmobranch, *Squalus acanthias*. Comp. Biochem. Physiol. *42*(A):3-12.

Gilmour, K.M., D.J. Randall, and S.F. Perry (1994). Acid-base disequilibrium in the arterial blood of rainbow trout. Respir.Physiol. *96*:259-272.

Gluck, S., and R. Nelson (1992). The role of the V-ATPase in renal epithelial H^+ transport. J. exp. Biol. *172*:205-218.

Gluck, S.L., R.D. Nelson, B.S. Lee, Z.-Q. Wang, X.-L. Guo, J.-Y. Fu, and K. Zhang (1992). Biochemistry of the renal V-ATPase. J. exp. Biol. *172*:219-229.

Goss, G., S. Perry, and P. Laurent (1995) Ultrastructural and morphometric studies on ion and acid-base transport processes in freshwater fish. In: Cellular and Molecular Approaches to Fish Ionic Regulation. Academic Press,, Vol. XIV, pp. 257-284.

Gros, G. (1991) The role of carbonic anhydrase within the tissues, with a special reference to mammalian striated muscle. In: Physiological Strategies for Gas Exchange and Metabolism. A.J. Woakes, M.K. Grieshaber, and C.R. Bridges, eds. Cambridge University Press, Cambridge, pp. 35-54.

Gros, G., W. Moll, H. Hoppe, and H. Gros (1976). Proton transport by phosphate diffusion- A mechanism of facilitated CO_2 transfer. J. Gen. Physiol. *67*:773-790.

Hansson, H.P.J. (1967). Histochemical demonstration of carbonic anhydrase activity. Histochemie *11*:112-128.

Harvey, B.J. (1992). Energization of sodium absorption by the H^+-ATPAse pump in mitochondria-rich cells of frog skin. J. exp. Biol. *172*:289-309.

Haswell, M.S., and D.J. Randall (1976). Carbonic anhydrase inhibitor in trout plasma. Respir.Physiol. *28*:17-27.

Heisler, N. (1988) Acid-base regulation. In: Physiology of the Elasmobranch Fishes. T.J. Shuttleworth, ed. Springer-Verlag, Berlin, pp. 215-252.

Heming, T.A., C. Geers, G. Gros, A. Bidani, and E.D. Crandall (1986). Effects of dextran-bound inhibitors on carbonic anhydrase activity in isolated lungs. J.Appl.Physiol. *61*:1849-1856.

Henry, R.P., S.J. Dodgson, R.E. Forster, and B.T. Storey (1986). Rat lung carbonic anhydrase: activity, localization and isozymes. J.Appl.Physiol. *60*:638-645.

Henry, R.P., N.J. Smatresk, and J.N. Cameron (1988). The distribution of branchial carbonic anhydrase and the effects of gill and erythrocyte carbonic anhydrase inhibition in the channel catfish *Ictalurus punctatus*. J. exp. Biol. *134*:201-218.

Henry, R.P., R.G. Boutilier, and B.L. Tufts (1995). Effects of carbonic anhydrase inhibition on the acid base status in lamprey and trout. Respir.Physiol. *99*:241-248.

Hill, E.P., G.G. Power, and R.D. Gilbert (1977). Rate of pH changes in blood plasma in vitro and in vivo. J.Appl.Physiol. *42*:928-934.

Hodler, J., H.O. Heinemann, A.P. Fishman, and H.W. Smith (1955). Urine pH and carbonic anhydrase activity in the marine dogfish. Am. J. Physiol. *183*:155-162.

Holder, L.B., and S.L. Hayes (1965). Diffusion of sulfonamides in aqueous buffers and into red cells. Mol. Pharmacol. *1*:266-279.

Jensen, F.B. (1989). Hydrogen ion equilibria in fish haemoglobin. J. exp. Biol. *143*:225-234.

Kent,B., and E.C. Pierce II (1978). Cardiovascular response to changes in blood gases in dogfish shark, *Squalus acanthias*. Comp. Biochem. Physiol. C *60*:37-44.

Klocke, R.A. (1978). Catalysis of CO_2 reactions by lung carbonic anhydrase. J.Appl.Physiol. *44*:882-888.

Klocke, R.A. (1980). Carbonic anhydrase in lung tissue. In: Biophysics and Physiology of Carbon Dioxide. C. Bauer, G. Gros, and H. Bartels, eds. Springer-Verlag, Berlin, pp. 331-338.

Kranovsky, M.J. (1965). A formaldehyde-glutaraldehyde fixative of high osmolarity for use in electron microscopy. J. Cell. Biol. *27*: 138A (Abstr.).

Lacy, E.R. (1983). Histochemical and biochemical studies of carbonic anhydrase activity in the opercular epithelium of the eurhaline teleost, *Fundulus heteroclitus*. Am. J. Anat. *166*:19-39.

Laemmli, U.K. (1970). Cleavage of structural proteins during the assembly of the head bacteriophage T4. Nature *227*:680-685.

Larsen, E.H. (1991). Chloride transport by high-resistance heterocellular epithelia. Physiol. Rev. *71*:235-283.

Larsen, E.H., N.J. Willumsen, and B.C. Christoffersen (1992). Role of proton pump of mitochondria-rich cells for active transport of chloride ions in toad skin epithelium. J. Physiol. *450*:203-216.

Laurent, P. (1984) Gill internal morphology. In: Fish Physiology. W. Hoar, and D.J. Randall, eds. Academic Press, New York, Vol. XA, pp. 73-183.

Laurent, P., and S. Dunel (1980). Morphology of gill epithelia in fish. Am. J. Physiol. *238*:R147-R159.

Laurent, P., G.G. Goss, and S.F. Perry (1994). Proton pumps in fish gill pavement cells? Arch. Int. Physiol. Biochim. Biophys. *102*:77-79.

Lessard, J., A.L. Val, S. Aota, and D. Randall (1995). Why is there no carbonic anhydrase activity available to fish plasma? J. exp. Biol. *198*:31-38.

Lin, H., and D. Randall (1991). Evidence for the presence of an electrogenic proton pump on the trout gill epithelium. J. exp. Biol. *161*:119-134.

Lin, H., and D.J. Randall (1993). H^+-ATPase activity in crude homogenates of fish gill tissue: inhibitor sensitivity and environmental and hormonal regulation. J. exp. Biol. *180*:163-174.

Lin, H., and D. Randall (1995) Proton Pumps in Fish Gills. In: Cellular and Molecular Approaches to Fish Ionic Regulation. Academic Press,, Vol. XIV, pp. 229-255.

Lin, H., D.C. Pfeiffer, A.W. Vogl, J. Pan, and D.J. Randall (1994). Immunolocalization of proton-ATPase in the gill epithelia of rainbow trout. J. exp. Biol. *195*:169-183.

Lönnerholm, G. (1982). Pulmonary carbonic anhydrase in the human, monkey, and rat. Am. J. Physiol. *52*:352-356.

Lönnerholm, G., and P.J. Wistrand (1984). Carbonic anhydrase in the human kidney: A histochemical and immunocytochemical study. Kidney Int. *25*:886-898.

Low, M., J. Stiernberg, G.L. Waneck, R.A. Flavell, and P.W. Kincaide (1988). Cell-specific heterogeneity insensitivity of phosphatidylinositol anchored membrane antigens to release by phospholipase C. J. Immunol. Methods *113*:101-111.

Madsen, K.M., and C.C. Tisher (1985). Structure-function relationships in H^+-sectreting epithelia. Federation Proc. *44*:2704-2709.

Maren, T.H. (1984). The general physiology of reactions catalyzed by carbonic anhydrase and their inhibition by sulfonamides. Ann. N.Y. Acad. Sci. *429*:568-579.

Maren, T.H., B.R. Friedland, and R.S. Rittmaster (1980). Kinetic properties of primative vertebrate carbonic anhydrases. Comp. Biochem. Physiol. *67*(B):69-74.

Maynard, J.R., and J.E. Coleman (1971). Elasmobranch carbonic anhydrase: purification and properties of the enzyme of two species of shark. J.Biol.Chem. *246*:4455-4464.

McLean, I.W., and P.K. Nakane (1974). Periodate-lysine-paraformaldehyde fixative. A new fixative for immunoelectron mircoscopy. J. Histochem. Cytochem. *22*:1077-1083.

Metcalfe, J.D., and P.J. Butler (1986). The functional anatomy of the gills of the dogfish (*Scyliorhinus canicula*). J. Zool. *208*:519-530.

Morgan, I.P., W.T.W. Potts, and K. Oates (1994). Intracellular ion concetrations in branchial epithelial cells of brown trout (*Salmo trutta* L.) determined by x-ray microanalysis. J. exp. Biol. *194*:139-151.

Nikinmaa, M., K. Tithonen, and M. Paajaste (1990). Adrenergic control of red blood cell pH in salmonid fish: roles of the sodium/ proton exchange, Jacobs-Stewart cycle and membrane potential. J. exp. Biol. *154*:257-271.

Nishimura, H. (1977). Renal responses to diuretic drugs in freshwater catfish *Ictalurus punctatus*. Am. J. Physiol. *232*:F278-F285.

Obaid, A.L., A. McElroy Critz, and E.D. Crandall (1979). Kinetics of bicarbonate / chloride exchange in dogfish erythrocytes. Am. J. Physiol. *237*:R132-R138.

Olson, K.R., and B. Kent (1980). The microvasculature of the elasmobranch gill. Cell Tissue Res. *209*:49-63.

Pan, J., D.C. Pfeiffer, C.L. Reimer, B.J. Crawford, A.W. Vogl, and N. Auersperg (1993). Lack of inter-species reactivity between antigens and antibodies is overcome by protease treatment of Western blots. Electrophoresis *14*:892-898.

Payan, P., and J. Maetz (1973). Branchial sodium transport mechanisms in *Scyliorhinus canicula*: evidence for Na^+/NH_4^+ and Na^+/H^+ exchanges and for a role of carbonic anhydrase. J. exp. Biol. *58*:487-502.

Payne, J.A., and D.H. Evans (1988). Anion transport in red cells of the dogfish shark, *Squalus acanthias*. Bull. Mt. Desert Isl. Biol. Lab. *27*:67-69.

Perry, S.F. (1986). Carbon dioxide excretion in fishes. Can. J. Zool. *64*:565-572.

Perry, S.F., and P. Laurent (1990) . In: Animal Nutrition and Transport Processes. 2. Transport, Respiration and Excretion: Comparative and Environmental Aspects. J.-P. Truchot, and B. Lahlou, eds. Comparative Physiology, Basel,Karger, Vol. 6.

Perry, S.F., P.S. Davie, C. Daxboeck, and D.J. Randall (1982). A comparison of CO_2 excretion in a spontaneously ventilating blood-perfused trout preparation and saline-perfused gill preparations: contribution of the branchial epithelium and red blood cell. J. exp. Biol. *101*:47-60.

Pfeiffer, D.C., and A.W. Vogl (1991). Evidence that vinculin is co-distributed with actin bundles in ectoplasmic ("juctional") specializations of mammalian sertoli cells. Anat. Rec. *231*:89-100.

Piiper, J., and P. Scheid (1984) Model analysis of gas transfer in fish gills. In: Fish Physiology. W.S. Hoar, and D.J. Randall, eds. Academic Press, New York, Vol. XA, pp. 229-262.

Piiper, J., and D. Schumann (1967). Efficiency of O_2 exchange in the gills of the dogfish, *Scyliorhinus stellaris*. Respir.Physiol. *2*:135-148.

Potts, W.T.W. (1994). Kinetics of sodium uptake in freshwater animals: a comparison of ion-exchange and proton pump hypotheses. Am. J. Physiol. *266*:R315-R320.

Rahim, S.M., J.-P. Delaunoy, and P. Laurent (1988). Identification and immunocytochemical localization of two different carbonic anhydrase isoenzymes in teleostean fish erythrocytes and gill epithelia. Histochem. *89*:451-459.

Riestenpatt, S., G. Petrausch, and D. Siebers (1995). Cl^- influx across posterior gills of the chinese crab (*Eriocheir sinensis*): potential energization by a V-type H^+-ATPase. Comp. Biochem. Physiol. *110A*:235-241.

Riordan, J.R., B. Forbush III, and J.W. Hanrahan (1994). The molecular basis of chloride transport in shark rectal gland. J. exp. Biol. *196*:45-418.

Rispens, P., J. Hessels, A. Zwart, and W.G. Zijlstra (1985). Inhibition of carbonic anhydrase in dog plasma. Pflügers Arch. *403*:344-347.

Rispens, R., B. Oeseburg, J.P. Zock, and W.G. Zijlstra (1980). Intra-aortic decrease in blood plasma pH. Pflügers Arch. *386*:97-99.

Ryan, U.S., P.L. Whitney, and J.W. Ryan (1982). Localization of carbonic anhydrase on pulmonary artery endothelial cells in culture. J.Appl.Physiol. *53*:914-919.

Scharschmidt, B.F., E.B. Keefe, N.M. Blankenship, and R.K. Ockner (1979). Validation of a recording spectrophotometeric method for measurement of membrane associated Mg^- and NaK-ATPase activity. J. Lab. Clin. Med. *93*:790-799.

Schultz, J.S. (1980) Facilitation of CO_2 through layers with a spatial distribution of carbonic anhydrase. In: Biophysics and Physiology of Carbon Dioxide. C. Bauer, G. Gros, and H. Bartels, eds. Springer-Verlag, Berlin, pp. 15-22.

Schwartz, G.J., and Q. Al-Awqati (1985). Carbon dioxide causes exocytosis of vesicles containing H^+ pumps in isolated perfused proximal and collecting tubules. J. Clin. Invest. *75*:1638-1644.

Shuttleworth, T.J. (1988) Salt and water balance -extrarenal mechanisms. In: Physiology of the Elasmobranch Fishes. T.J. Shuttleworth, ed. Springer-Verlag, Berlin, pp. 171-199.

Steinmetz, P.R. (1986). Cellular organization of urinary acidification. Am. J. Physiol. *251*:F173-F187.

Südhof, T.C., V.A. Fried, D.K. Stone, and P.A. Johnston (1989). Human endomembrane H^+ pump strongly resembles the ATP-synthetase of Archaebacteria. Proc. Natl. Acad. Sci. USA *86*:6067-6071.

Swenson, E.R. (1990). Kinetics of oxygen and carbon dioxide exchange. In: . R.G. Boutilier, ed. Springer-Verlag, Berlin, Vol. 6, pp. 163-210.

Swenson, E.R., M.A. Hildesley, and T.H. Maren (1982). The renal and branchial handling of CO_2 / HCO_3^- in the marine elasmobranch. Bull. Mt. Desert Isl. Biol. Lab. *22*:72-75.

Swenson, E.R., and D.H. Evans (1984). Inhibition of gill carbonic anhydrase blocks CO_2 excretion in the isolated perfused head of the dogfish 'pup' *Squalus acanthias*. Bull. Mt. Desert Isl. Biol. Lab. *24*:45-49.

Swenson, E.R., and T.H. Maren (1984). Effects of acidosis and carbonic anhydrase inhibition in the elasmobranch rectal gland. Am. J. Physiol. *247*:F87-F92.

Swenson, E.R., T.H. Maren, and M.A. Hildesley (1984). Further studies on elasmobranch CO_2 and HCO_3^- excretion: Roles of branchial and erythrocyte carbonic anhydrase in *Squalus acanthias*. Bull. Mt. Desert Isl. Biol. Lab. *24*:72-75.

Swenson, E.R., and T.H. Maren (1986). Dissociation of CO_2 hydration and renal acid secretion in the dogfish, *Squalus acanthias*. Am. J. Physiol. *250*:F288-F293.

Swenson, E.R., and T.H. Maren (1987). Roles of gill and red cell carbonic anhydrase in elasmobranch HCO_3^- and CO_2 excretion. Am. J. Physiol. *253*:R450-R458.

Swenson, E.R., L. Lippincott, and T.H. Maren (1995). Effect of gill membrane-bound carbonic anhydrase inhibition on branchial bicarbonate excretion in the dogfish shark, *Squalus acanthias*. Bull. Mt. Desert Isl. Biol. Lab. *34*:94-95.

Tokuyasu, K.T., and S.J. Singer (1976). Improved procedures for immunoferritin labeling of ultrathin frozen sections. J. Cell Biol. *71*:894-906.

Towbin, H., T. Staehelin, and J. Gordon (1979). Electrophoretic transfer of proteins from polyacrylamide gels to nitrocellulose sheets: procedure and some applications. Proc. Natl. Acad. Sci. USA *76*:4350-4354.

Tufts, B.L., and D.J. Randall (1989). The functional significance of adrenergic pH regulation in fish erythrocytes. Can. J. Zool. *67*:235-238.

Verlander, J.W., K.M. Madsen, P.S. Low, D.P. Allen, and C.C. Tisher (1988). Immunocytochemical localization of band 3 protein in the rat collecting duct. Am. J. Physiol. *255*:F115-F125.

Whitney, P.L., and T.V. Briggle (1982). Membrane-associated carbonic anhydrase purified from bovine lung. J.Biol.Chem. *257*:12056-12059.

Wistrand, P.J., and K.-G. Knuuttila (1989). Renal membrane-bound carbonic anhydrase. Purification and properties. Kidney Int. *35*:851-859.

Wood, C.M., S.F. Perry, P.J. Walsh, and S. Thomas (1994). HCO_3^- dehydration by the blood of an elasmobranch in the absence of a Haldane effect. Respir. Physiol. *98*:319-337.

Wright, D.E. (1973). The structure of the gills of the elasmobranch, *Scyliorhinus canicula* (L.). Z. Zellforsch *144*:489-509.

Zaugg, W.S. (1982). A simplified preparation for adenosine triphospate determination in gill tissue. Can. J. Fish. Aquat. Sci. *39*:215-217.

Zock, J.P., P. Rispens, and W.G. Zijlstra (1981). Calculated changes in pH and pCO_2 in arterial blood plasma assuming abscence of ion and water exchange between plasma and erythrocytes during their equilibration with alveolar gas. Pflügers Arch. *391*:159-161.